Combined Tension and Bending Loading in Bottom Chord Splice Joints of Metal-Plate-Connected Wood Trusses

by

Philip J. O'Regan

Thesis submitted to the Faculty of the

Virginia Polytechnic Institute and State University

in partial fulfillment of the requirements for the degree of

MASTER OF SCIENCE

in

Biological Systems Engineering

APPROVED:

Frank E. Woeste, Chairman

Joseph R. Loferski

Audrey G. Zink

John V. Perumpral

May, 1997

Blacksburg, Virginia

Keywords: wood truss, combined loading, truss plate, splice joints, truss design

Combined Tension and Bending Loading in Bottom Chord Splice Joints of Metal-Plate-Connected Wood Trusses

by

Philip J. O'Regan

Frank E. Woeste, Chair

Biological Systems Engineering

(ABSTRACT)

Metal-plate-connected (MPC) splice joints were tested in combined tension and bending to generate data that were used in the development of a design procedure for determining the steel net-section strength of bottom chord splice joints of MPC wood trusses. Several common wood truss splice joint configurations were tested at varying levels of combined tension and bending loading. The joint configurations were 2x4 lumber with 20-gauge truss plates, 2x6 lumber with 20-gauge truss plates, and 2x6 lumber with 16-gauge truss plates. All the joints tested failed in the steel net-section of the truss plates. The combined loading was achieved by applying an eccentric axial tension load to the ends of each splice joint specimen.

Three structural models were developed to predict the ultimate strength of the steel net-section of the splice joints tested under combined tension and bending loading. The test data were fitted to each model, and the most accurate model was selected. Data from other published tests of splice joints were used to validate the accuracy of the selected model. A design procedure for determining the allowable design strength of the steel net-section of a splice joint subjected to combined tension and bending was developed based on the selected model. The new design procedure was compared with two existing design methods. The proposed design procedure is recommended for checking the safe capacity of the steel net-section of bottom chord splice joints of MPC wood trusses subjected to combined tension and bending.

Acknowledgments

I thank the members of my graduate committee for their guidance and assistance throughout my research. The committee members were Drs. Frank Woeste, Joe Loferski, and Audrey Zink. I especially thank Frank Woeste for all of his advice, encouragement, criticism, and support during my education at Virginia Tech. Frank played a key role in my decision to pursue a Master's degree. He had confidence in my abilities, and for that I am grateful.

I thank Dr. Perumpral and the Biological Systems Engineering Department for their financial assistance. This support made my graduate education possible.

Special thanks go to Stuart Lewis, P.E., of Alpine Engineered Products, Inc., for providing invaluable technical advice, answers, and criticism. I appreciate the time and effort he gave to assist me with this research. Stu also provided truss plates for this study and test data on the mechanical properties of the steel coil used to manufacture the truss plates.

The help of Steve Spradlin, Bob Carner, Butch Sizemore, Carlile Price, and Terry Platt is gratefully acknowledged. Steve fabricated several fixtures used in the testing that I conducted. Bob and Butch assisted with the use of the testing machine, and Bob also explained the data acquisition equipment. Carlile helped me find the tools and equipment I needed. I thank Terry for sharing his knowledge of the testing machine, and for adjusting his schedule so we both could use the test equipment.

I thank my friends and fellow graduate students; their friendship and company will be missed long after I leave Blacksburg. Finally, I thank my sisters and parents for their support and encouragement.

Table of Contents

List of Figures

List of Tables

Notations

b	thickness of the truss chord lumber (in.)
C	ultimate compression parallel-to-grain strength of lumber (psi)
C_F	size factor for solid-sawn lumber
$\tilde{C}$	median value of the distribution of the ultimate compression parallel-to-grain strength of lumber (psi)
$C_{0.05}$	fifth percentile value of the distribution of the ultimate compression parallel-to-grain strength of lumber (psi)
d	depth of the truss chord lumber (in.)
e	initial eccentricity of the tension load applied to the test joint specimen (in.)
e_t	tension efficiency ratio of the truss plate
F_c	nominal allowable design strength for lumber in compression parallel-to-grain (psi)
F_u	ultimate tensile strength of the truss plate steel (psi)
F_y	tensile yield strength of the truss plate steel (psi)
F_{steel}	tensile resistive strength of the steel in tension (lb.)
F_{wood}	compressive resistive strength of wood under compression parallel-to-grain (lb.)
k	ratio of the median value of a distribution to the fifth percentile value
M	applied moment at splice joint (in.-lb.)
M_{all}	allowable moment that may be applied to the splice joint (in.-lb.)
$\overline{M}_e$	average ultimate moment at failure for the group of test joints with e inches of initial eccentricity (in.-lb.)
$M_{i,e}$	ultimate moment at failure for the i^{th} replicate of the test group with e inches of initial eccentricity (in.-lb.)
M_{ult}	ultimate moment capacity of the splice joint (in.-lb.)
$m_{i,e}$	standardized moment at failure for the i^{th} replicate of the test group with e inches of initial eccentricity
N.A.	neutral axis

s_e standard deviation of the ultimate moment at failure for the group of test joints with e inches of initial eccentricity (in.-lb.)

T applied tension load at splice joint (lb.)

T_{all} allowable tension load that may be applied to the splice joint (lb.)

$T_{all,M}$ allowable tension load that may be applied in addition to the applied moment (lb.)

$T_{all,T}$ allowable tension-only capacity of the splice joint (lb.)

$T_{all,Com}$ allowable tension load as calculated using the design method of the ANSI/TPI Commentary (lb.)

$T_{all,6}$ allowable tension load as calculated using the 6M/w design method (lb.)

T^* equivalent tension load that produces the same stress as the applied moment (lb.)

t thickness of the truss plate (in.)

w width of the truss plate (in.)

y distance from the truss chord centerline to the neutral axis (in.)

y^* distance from the truss chord centerline to the neutral axis for the moment-only case (in.)

Δ transverse deflection of the splice joint specimen at failure (in.)

1. Introduction

Metal-plate-connected (MPC) wood trusses can be found in a variety of building applications. Residential homes and apartments, franchise restaurants, and many agricultural, commercial, and industrial buildings use wood trusses because of their ease of construction and long-span capabilities. Based on estimates by industry leaders, almost 2,000 MPC wood truss manufacturers in the United States had a total gross sales of $3.4 billion in 1996.

Although metal-plate-connected (MPC) wood trusses have been widely used for over 30 years, the behavior of the metal plate connections is not fully understood. In fact, most of the research in the MPC wood truss industry has focused on modeling and predicting the strength of MPC wood truss joints. One particular joint that has not been widely researched is the tension splice joint found in the bottom chord of both pitched roof trusses and parallel chord roof trusses. Trusses with spans that exceed the length of commonly available lumber require splice joints to connect two (or more) pieces together. Figure 1.1 shows a bottom chord splice joint for a typical pitched roof truss, and Figure 1.2 shows a bottom chord splice joint for a typical parallel chord roof truss.

Metal connector plates are fabricated from coils of galvanized sheet steel with typical thicknesses of 16-gauge, 18-gauge, and 20-gauge (0.058, 0.047, and 0.036 in.). The plates are die-punched to form teeth protruding perpendicularly to the plate. Two pieces of lumber, usually 2-in. nominal thickness dimension lumber, are connected by pressing a pair of plates into the lumber, with one plate on each side of the joint. The plates must resist forces in the plane of the plate. These forces include tension, compression, shear, combined tension and shear, and combined compression and shear. MPC wood truss plates are available in a variety of sizes, gauges, and tooth configurations to suit many different joint configurations.

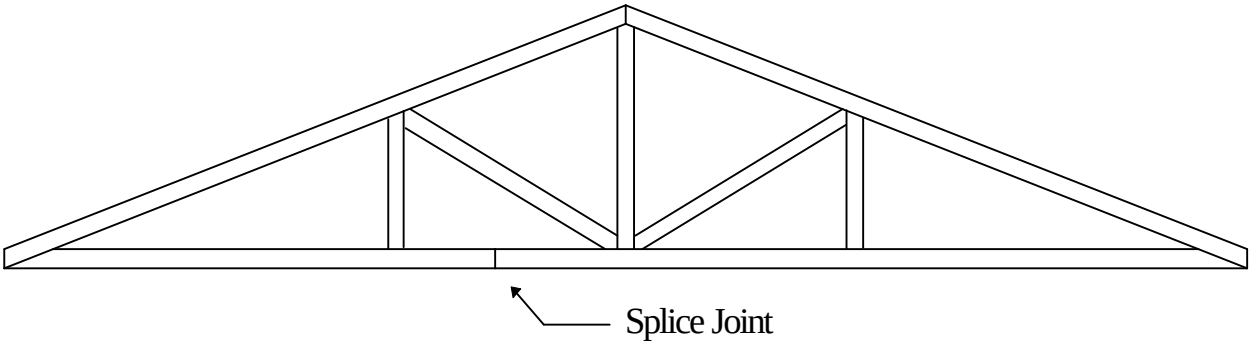

Figure 1.1 Typical bottom chord splice joint in a pitched roof truss.

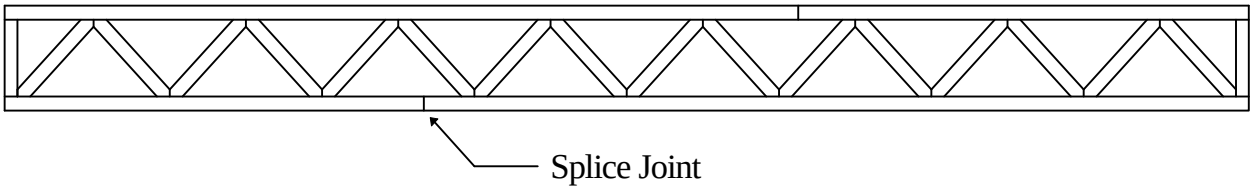

Figure 1.2 Typical bottom chord splice joint in a parallel chord roof truss.

1.1 Design of MPC Wood Trusses

The design of MPC wood trusses involves selecting the size, grade, and species (or species group) of lumber required to resist the applied loads, and designing the joints to transmit the forces developed in the lumber members. The truss joints may fail in one of three failure modes. Tooth withdrawal failure occurs when the teeth of the metal connector plate pull out from the lumber when subjected to a lateral load. The ability of the truss plate teeth to resist this type of failure mode is called "lateral resistance," and is expressed in units of force per unit area of plate contact area. Truss plates can also experience failures in the steel due to shear stresses. This failure mode is often found in the heel joints of pitched roof trusses where the top and bottom chords meet. The third failure mode for truss plates is failure of the net cross-section of the steel due to tension stresses. Common in bottom chord splice joints, this failure mode involves yielding and rupture of the steel due to tensile stresses produced by axial loads applied parallel to the length of the truss plate and bending moments at the joint.

For bottom chord splice joints, the two failure modes that a truss designer must check are tooth withdrawal and steel net-section failure. Usually bottom chord splice joints are located in areas such that they experience a small bending moment, and are stressed primarily in tension. For truss design in the United States, the effect of the moment on tooth withdrawal is generally not included in the design check for tooth withdrawal. According to industry practice, the effect of the bending moment on the steel net-section capacity may or may not be included in the design of a bottom chord splice joint. A design methodology for determining the steel net-section capacity of splice joints subjected to a bending moment as well as a tension load has not been adopted by the MPC wood truss industry.

1.2 Objectives

The main objective of this research is to develop a design method for determining the steel net-section capacity of bottom chord splice joints of MPC wood trusses subjected to combined tension and moment loading. Actual splice joints were tested to generate data for the development of a model to predict the combined tension and moment capacity of the steel net-section. In addition, results of previous studies of combined loading of tension splice joints will be used to validate the model. Based on the model, a procedure for determining the design capacity of the steel net-section of a splice joints subjected to combined tension and bending will be proposed. Finally, some recommendations for a standard method of testing splice joints in combined tension and bending will be given.

2. Literature Review

2.1 Current Design Methods

As early as 1966, it was noted in the research literature that tension splice joints in the bottom chords of MPC wood trusses may be subjected to combined bending and tension forces. Dudley (1966) emphasized the importance of the steel net-section as a limit state for metal connector plates, especially for bottom chord splice joints that must carry a bending moment in addition to a tension force.

Truss design in the United States follows the guidelines of the ANSI/TPI 1-1995 National Design Standard for Metal Plate Connected Wood Truss Construction, a standard developed by TPI, the Truss Plate Institute (TPI, 1995a). This standard includes procedures for designing the members and joints of MPC wood trusses. Section 11.2.5 addresses combined flexure (bending) and axial loading of truss joints. This section states:

> Splices in the top and bottom chords located within 12 inches of the calculated point of zero moment shall be permitted to have metal connector plates designed for axial forces only. Design of inter-panel splices in the top or bottom chord not located within 12 inches of the calculated point of zero moment shall include the additional stress caused by flexure.

However, the standard does not provide a method for incorporating the additional stress caused by the moment into the joint design check for steel net-section. The commentary to ANSI/TPI 1-1995 suggests a "conservative approach" to this problem (TPI, 1995b). Essentially, the approach is to convert the applied moment, M, into an equivalent tension force, T^*, which can then be added to the applied axial tension, T (T and M are found from the truss analysis). The resulting total tension force is then used to design the steel net-section of the joint. The ANSI/TPI commentary does not provide a design equation for this method; only a design example is given, and the equation is implied in the example. Equation 2.1 shows how the equivalent force is calculated:

$$T^* = \frac{3M}{2d} \tag{2.1}$$

where d is the depth of the wood member. This method has not been validated by any published laboratory test reports. The derivation of this design method is given in Appendix A.

Another method used by some truss designers is similar to the suggested method given in the ANSI/TPI Commentary. Again, the applied moment, M, is converted into an equivalent force, T^*. Equation 2.2 shows how this force is calculated:

$$T^* = \frac{6M}{d} \tag{2.2}$$

where d is the depth of the wood member. As with the suggested method of the ANSI/TPI Commentary, this design method has not been validated by any published laboratory test reports. It is interesting to note that the equivalent tension force calculated using Equation 2.2 is four times that calculated by Equation 2.1.

Whale (1993) briefly summarized the truss plate design procedures used in the United Kingdom. He noted that "no attempts are generally made to design plates for internal eccentricity moments or external moments." If splice joints are positioned in low moment areas, such as near panel points, then they are assumed to be rigid joints (i.e., the truss chord is treated as a continuous member). The effect of moments in these low moment areas is incorporated into the plate design by empirically adjusting the axial forces in the chord member. Whale did not discuss how the axial forces are adjusted. In addition, it is not clear if the adjustment of the axial forces applies to the tooth withdrawal capacity or the steel net-section capacity (or both) of the splice joint.

Eurocode 5, the voluntary design code for timber structures in Europe, does consider moments in the design of truss plates (Whale, 1993). The applied moment is resolved into a force couple. This force couple is incorporated into Equation 2.3, which is then used to determine the capacity of the steel net-section of a truss plate:

$$\left(\frac{F_x}{R_{x,d}}\right)^2 + \left(\frac{F_y}{R_{y,d}}\right)^2 \leq 1 \tag{2.3}$$

where:

F_x is the force component acting parallel to the length of the truss plate,
F_y is the force component acting parallel to the width of the truss plate,
$R_{x,d}$ is the capacity of the truss plate parallel to the length, and
$R_{y,d}$ is the capacity of the truss plate parallel to the width.

When the design procedures of Eurocode 5 for steel net-section are applied to a bottom chord splice joint, Equation 2.3 can be reduced to Equation 2.4:

$$\left(\frac{T}{2tw(0.6F_y)e_t}\right)^2+\left(\frac{4M/w}{2tw(0.577F_u)e_v}\right)^2\le 1 \qquad (2.4)$$

where:

T is the applied axial force,
M is the applied moment,
t is the thickness of the truss plate,
w is the width of the truss plates,
F_y is the tensile yield strength of the truss plate steel,
F_u is the ultimate tensile strength of the truss plate steel,
e_t is the tension efficiency ratio for the truss plates, and
e_v is the shear efficiency ratio for the truss plates.

The denominator of the second term on the left side of Equation 2.4 represents the allowable shear strength of the truss plates. Since splice joints are not subjected to significant shear, as a heel joint would experience, it is not logical to consider the shear strength of the truss plates when designing splice joints. Therefore, Equation 2.3 is not a desirable option for determining the design capacity of the steel net-section of splice joints subjected to combined tension and bending.

2.2 Testing Standards

Testing standards for MPC joints in the United States are published by TPI in ANSI/TPI 1-1995. Standard test methods are given for determining the design strength of metal connector plates for three failure modes: lateral resistance strength of metal connector plate teeth (tooth withdrawal), strength of the steel net-section of connector plates under shear forces, and strength of the steel net-section of connector plates under pure tension forces. No standard test method is given for determining the lateral resistance strength or the steel net-section strength of connector plates under combined tension and bending loading.

The need for design methodologies and test standards for combined loading of MPC wood trusses has been recognized (ASCE, 1986). Gupta et al. (1996) suggested that most current design standards oversimplify the actual loading conditions of MPC joints. Further, they noted that no standards exist “for testing actual configurations of MPC joints….under simulated, in-service loading conditions (e.g., combined bending and tension).” Wolfe et al. (1991) suggested that the first step in developing an acceptable design methodology for combined loading is to adopt a standard test procedure.

Section 7.1 of ANSI/TPI 1-1995, "Standard Method of Test for Strength Properties of Metal Connector Plates Under Pure Tension Forces," describes the procedures for determining the steel net-section capacity of truss plates. Although applicable to tension-only loading, this test method can be used as the basis for a standard method for testing the steel net-section of splice joints in combined tension and bending loading. Therefore, a brief summary of this method follows.

2.2.3 Summary of ANSI/TPI 1-1995, Section 7.3, Standard Method of Test for Strength Properties of Metal Connector Plates Under Pure Tension Forces

Procedures are given for testing both punched truss plates and solid metal control specimens. The testing machine used must have parallel, self-centering grips. This ensures that only axial tension loading will occur. The truss plates used must be typical production plates, and the mechanical properties of the steel coil used to manufacture the plates must meet the requirement for the specified steel grade. A minimum of three solid metal control specimens from the steel coil must be tested following ASTM Standard E8 (ASTM, 1996a). The test specimens must be assembled in the same manner as actual trusses, and the plates must be firmly embedded into the lumber. The plates must be long enough to induce steel net-section failures, rather than tooth withdrawal failures. A minimum of six test specimens must be tested. The tests must be conducted such that failure occurs in three to five minutes.

2.3 Previous Studies

While the structural performance of MPC wood trusses has being extensively researched, few studies involving combined tension and bending loading of truss joints have been conducted. However, the test data from previous studies of combined loading of splice joints can be used, in addition to the test data generated in this study, for evaluating the models that are presented later. Also, all published studies of the moment capacity of MPC joints will be considered.

Wolfe (1990) tested the capacity of MPC wood truss splice joint connections for five combinations of bending and tension loading. Test specimens of 2x4 Southern Pine lumber and 3- by 5.25-in. 20-gauge truss plates were tested in tension only, bending only, and three levels of combined loading. The manufacturer of the truss plates and the grade of the lumber used in this study were not reported. The combined loading was achieved with a specially designed testing apparatus described in Wolfe et al. (1991). The combined loading test results demonstrated that the tension capacity of the joint decreased as the applied moment increased, as shown in Table 2.1. An interaction equation was derived for the splice joint configuration used in this study. Equation 2.5 was the proposed interaction equation:

$$\frac{t}{T} + \frac{m^a}{M} \leq 1 \qquad (2.5)$$

where:

t is the applied axial tension force,
T is the tension capacity of the steel net-section of the pair of truss plates,
m is the applied bending moment,
M is the moment capacity of the steel net-section of the pair of truss plates, and
a is an exponent derived from test results.

This interaction equation requires two parameters that can be determined only from tests of truss plates: the moment capacity of the steel net-section, M; and the exponent, a. To use this equation for design purposes, each different truss plate design (tooth pattern, tooth geometry, and steel grade) must be tested to determine these two parameters. For the truss plates used in his study, Wolfe determined a value of 1.28 for the exponent, a.

Table 2.1 Wolfe (1990) results from testing splice joints in combined loading.

Applied Loading Level	Number of Tests	Tension Load[a] (lbs.)	Tension COV[b] (%)	Moment[a] (in.-lb.)	Moment COV[b] (%)
Tension only	20	6,700	6	----	----
Low moment, high tension	10	4,800	7	3,330	9
Medium moment and tension	10	2,530	5	6,040	3
High moment, low tension	12	940	5	7,110	5
Moment only	10	----	----	8,680	6

[a]The tabulated tension loads and bending moments were measured at joint failure.
[b]Coefficient of variation.

Gupta (1994) tested tension splice joints under six loading conditions. Axial tension only, bending only, and four levels of combined tension and bending loading were applied to joints fabricated using 2x4 No. 2 KD19 Southern Pine lumber and 3- by 4-in. 20-gauge Alpine truss plates manufactured by Alpine Engineered Products, Inc. An axial load was applied to the test specimens using wood-gripping friction plates. Each friction plate had a column of holes drilled in the end, allowing eccentric loading. The moment-only loading was accomplished with third-point

bending. Most of the specimens tested failed in tooth-withdrawal. A few specimens failed with a combination of steel failure and tooth withdrawal; on one side of the joint, the plate failed in steel net-section, and on the other side the plate failed in tooth-withdrawal. Only one specimen failed in steel net-section of both truss plates. Gupta derived an interaction equation (Equation 2.6) for determining the tooth withdrawal capacity for combined tension and bending of the joints tested:

$$\left(\frac{t}{T}\right)^{a} + \left(\frac{m}{M}\right)^{b} \leq 1 \qquad (2.6)$$

where:

t is the applied axial tension force,
T is the tooth withdrawal capacity of the pair of truss plates,
m is the applied bending moment,
M is the moment capacity for tooth withdrawal of the pair of truss plates, and
a and b are exponents derived from test results.

The values of the parameters a and b for the plates used in his study were 8.3011 and 0.6083, respectively. Gupta concluded that the tooth withdrawal capacity of MPC joints decreases as the applied moment increases.

Noguchi (1980) studied the maximum bending moment capacity of the steel net-section of spliced butt joints loaded in pure bending, with truss plates located above the centerline of the wood members. Because the truss plates were located above the neutral axis, they were stressed in tension only, and did not experience compression buckling. The wood fibers of the truss chord below the neutral axis carried the compressive stress component of the applied bending moment.

Noguchi presented five models to predict the moment capacity of the steel net-section of the joints, and fitted test data to determine which model was the most accurate. Noguchi's Model 1 was an elastic model based on the assumption that both the steel of the truss plate and the wood of the truss chord behave elastically. Model 2 was based on elastic behavior for the steel, and plastic behavior for the wood. Model 3 was based on plastic behavior for the steel, and elastic behavior for the wood. Model 4 was based on plastic behavior for both the steel and the wood. The fifth model was originally presented by Edlund (1971, as quoted by Noguchi, 1980), and was based on the assumption that the neutral plane was located at one-third of the height of the wood member when a joint is yielding. Noguchi concluded that Model 4, the plastic model, was the most accurate model. He suggested that this model be used to calculate the ultimate moment capacity of the steel net-section of butt joints with truss plates located above the neutral axis.

Kevarinmäki (1996) studied the anchorage (tooth withdrawal) capacity of MPC wood truss joints subjected to moments, using both elastic and plastic theory models. He presented simplified

methods for determining the force and moment components acting on the truss plates of a splice joint loaded in bending and tension (or compression) for checking the tooth withdrawal capacity of the joint. However, he did not discuss the steel net-section capacity of splice joints subjected to combined loading.

Soltis (1985) tested several configurations of truss plate splice joints in bending-only as part of a study of partially continuous floor joists. Three connection types were used to form continuous floor joists; glued plywood side plates, finger joints, and truss plates. The constructed joists were tested in bending using third-point loading. Three sizes of several species groups of No. 2 and Better lumber were used with truss plates fabricated from 16-gauge ASTM A446 Grade A steel (ASTM, 1994) (the plate manufacturer was not reported). Descriptions of the joint configurations tested are given in Table 2.2. Five test specimens of each combination of lumber size and species group were loaded to failure in bending. Most of the Douglas Fir-Larch and Spruce-Pine-Fir specimens failed in the steel net-section of the truss plates. All of the White Woods specimens had failures other than steel net-section failures. Although Soltis's study tested MPC joints in bending-only, the test data can be used to evaluate the models developed later in this study.

Table 2.2 Soltis (1985) results from testing splice joints in bending.

Species Group	Joist Size	Truss Plate Size width-length (in.)	Number of Steel Net-section Failures	Average[a] Moment (in.-lb.)	COV[b] Moment (%)
Douglas Fir-Larch	2x6	5 x 20	5	34,980	4.2
	2x8	7 x 14	3	79,500	4.2
	2x10	9 x 18	2	121,860	3.4
Spruce-Pine-Fir	2x6	5 x 14	5	32,976	4.3
	2x8	7 x 12	2	70,380	23
White Woods	2x10	9 x 12	0	----	----

[a]The average ultimate moment includes only the specimens for each group that failed in steel net-section.
[b]Coefficient of variation.

3. Experimental Materials and Methods

To provide data for the development of a structural model for combined tension and bending loading of the steel net-section of truss splice joints, actual splice joints were fabricated and tested to failure under combined tension and bending loading. The joint configurations selected are commonly found in many wood truss applications. The lumber used for the test specimens was No. 2 KD19 Southern Pine, in both 2x4 and 2x6 nominal sizes.

Because of the high stress levels common in bottom chord splice joints, truss plates chosen for splice joints usually have high steel net-section capacities, which can be achieved either by using thicker plates (e.g., 16-gauge) or by using high-strength steel (e.g., Grade 60). The truss plates used for the 2x4 test specimens were Alpine HS2510 truss plates, made from 20-gauge ATSM A653 HSLA Grade 60 steel (ASTM, 1996b). For the 2x6 specimens, two types of plates were used: Alpine HS412 plates of 20-gauge ASTM A653 HSLA Grade 60 steel; and Lumbermate K510 plates of 16-gauge ASTM A653 SQ Grade 37 steel. Plate lengths were chosen to prevent tooth withdrawal failures, since the objective was to study steel net-section strength. Alpine Engineered Products, Inc., supplied the truss plates. Table 3.1 gives a summary of the properties of the truss plates used in this study, and a photograph of the truss plates is shown in Figure 3.1.

All of the 20-gauge plates for the 2x4 and 2x6 lumber specimens were punched from the same coil of ASTM A653 HSLA Grade 60 steel. All of the 16-gauge plates were made from the same coil of ASTM A653 SQ Grade 37 steel. The steel mill that supplied the steel coils provided steel certificates that listed the yield and ultimate strength properties of the steel as determined by tests conducted by the mill. In addition to the mill's tests, the truss plate manufacturer conducted ASTM E8 tensile tests using three punched coupons from the solid steel coils used to produce the truss plates. Table 3.2 shows a comparison of the strength properties of the steel coil used to make the truss plates used in this study. The nominal yield and ultimate strength values are the ASTM minimum strengths for that grade of steel.

Table 3.1 Properties and dimensions of the truss plates used for the joint tests.

Truss Plate[a]	Steel Grade	Gauge (thickness) (in.)	Width (in.)	Length (in.)	Tooth Density (teeth/in^2)	Tooth Pattern
Alpine HS2510	60[b]	20 (0.0356)	3.28	8.75	6.97	Staggered
Alpine HS412	60	20 (0.0356)	5.25	10.5	6.97	Staggered
Lumbermate K510	37[c]	16 (0.0575)	5.0	10.5	4.57	Partially Staggered

[a]The plates used in this study are described in SBCCI PST & ESI Evaluation Report No. 94168 (1995).
[b]ASTM A653 HSLA Grade 60 steel (ASTM, 1996b)
[c]ASTM A653 SQ Grade 37 steel (ASTM, 1996b)

Table 3.2 Summary of yield and ultimate strength properties from coupon tests for the steel coils used to manufacture the test truss plates, as reported by the steel supplier and the plate manufacturer.

Steel Grade	Steel Gauge	Tensile Yield Strength (F_y)			Ultimate Tensile Strength (F_u)		
		Nominal (ksi)	Steel Mill (ksi)	Manufacturer (ksi)	Nominal (ksi)	Steel Mill (ksi)	Manufacturer (ksi)
ASTM A653 HLSA Grade 60	20	60	56.9	58.9	70	72.9	74.1
ASTM A653 SQ Grade 37	16	37	46.9	54.5	52	57.9	59.5

Both the steel supplier and the plate manufacturer reported that the yield strength of the test coupons for the Grade 60 steel used for the 20-gauge plates was below the ATSM specified minimum yield strength for Grade 60 steel. However, the average ultimate strength of the test coupons was greater than the ASTM specified minimum ultimate strength. Although the nominal yield strength is used to calculate the allowable design strength for the steel net-section, the steel net-section will not fail until the ultimate strength is reached. Therefore, the 20-gauge truss plates used in this study did not bias the results of the tests because the model subsequently developed and recommended for design is based on the ultimate strength of the steel, not the yield strength.

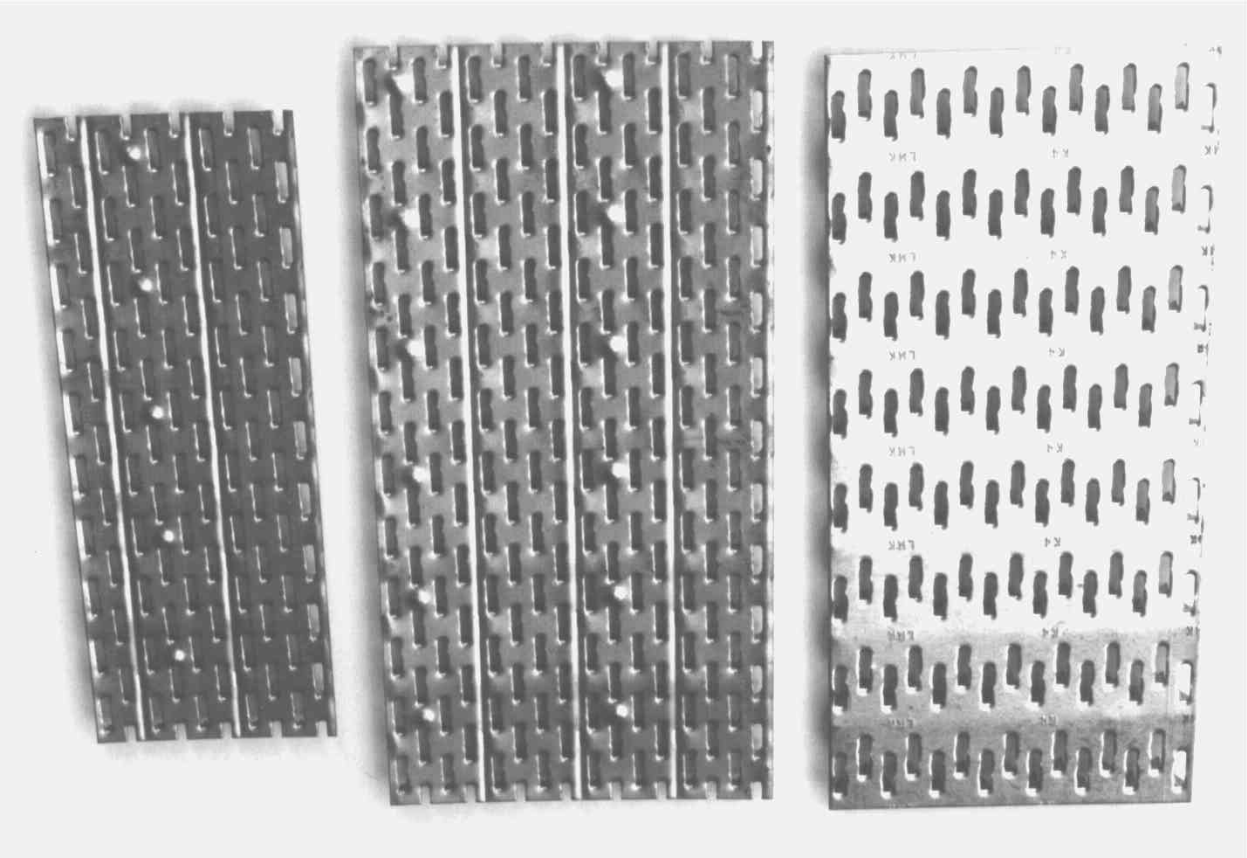

Figure 3.1 **Photograph of the truss plates used in this study. Shown from left to right are an Alpine HS2510 20-gauge truss plate, an Alpine HS412 20-gauge truss plate, and a Lumbermate K510 16-gauge truss plate.**

3.1 Design of Grip Plates

To produce both tension and bending stresses in a member, an eccentric axial load can be applied to both ends of the member. This approach was used in this study to produce the combined stresses in the splice joints tested. A pair of ASTM A36 ¼-in. steel plates were bolted to each end of the test specimens using four ASTM A307 ¾-in. diameter bolts. Two sets of grip plates were used; one set was for use with 2x4 lumber, and the other was for use with 2x6 lumber.

The grip plates for the 2x4 lumber specimens had a row of four 1-in. diameter holes at the ends of the grip plates for attaching the grip plates to the testing machine. The first hole was in-line with the centerline of the lumber. When this hole was used to attach both ends of the test specimen to the testing machine, a centric load resulted and therefore only tension stresses were produced in the joint. Using the second hole resulted in a load eccentricity of 1.5 in., thereby producing both tension and bending stresses in the joint. The third and fourth holes produced load eccentricities of 3 and 4.5 in., respectively. Figure 3.2 is a diagram of a 2x4 test joint with the grip plates bolted attached. Figure 3.3 shows how an eccentrically applied tension load produces both a tension force and a bending moment in the splice joint.

The grip plates for the 2x6 lumber specimens were similar to the 2x4 grip plates, except that they only had three attachment holes. Using the first hole resulted in centric loading. The second and third holes produced load eccentricities of 1.5 and 3.5 in., respectively. Figures 3.4 and 3.5 show the dimensions of the 2x4 and 2x6 grip plates.

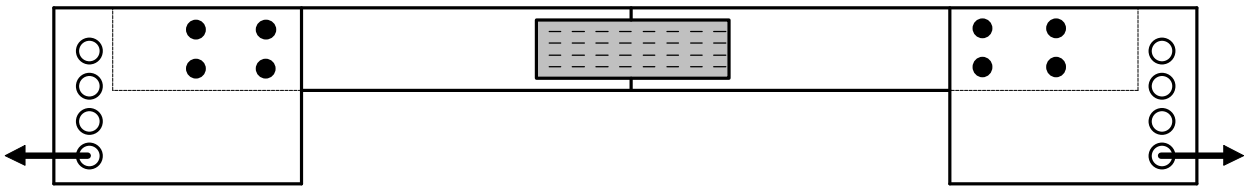

Figure 3.2 2x4 test joint with grip plates bolted onto each end.

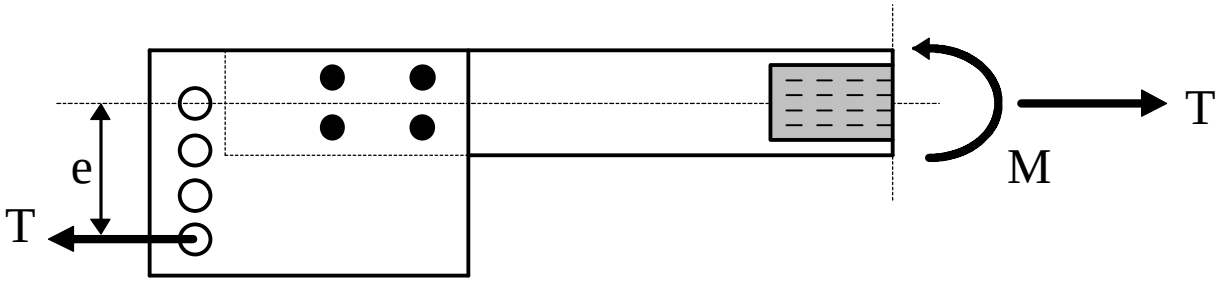

Figure 3.3 **Tension and bending stresses were produced by applying a tension load, T, at a selected eccentricity, e. The moment, M, was calculated as the eccentricity, e, at failure, times T at failure.**

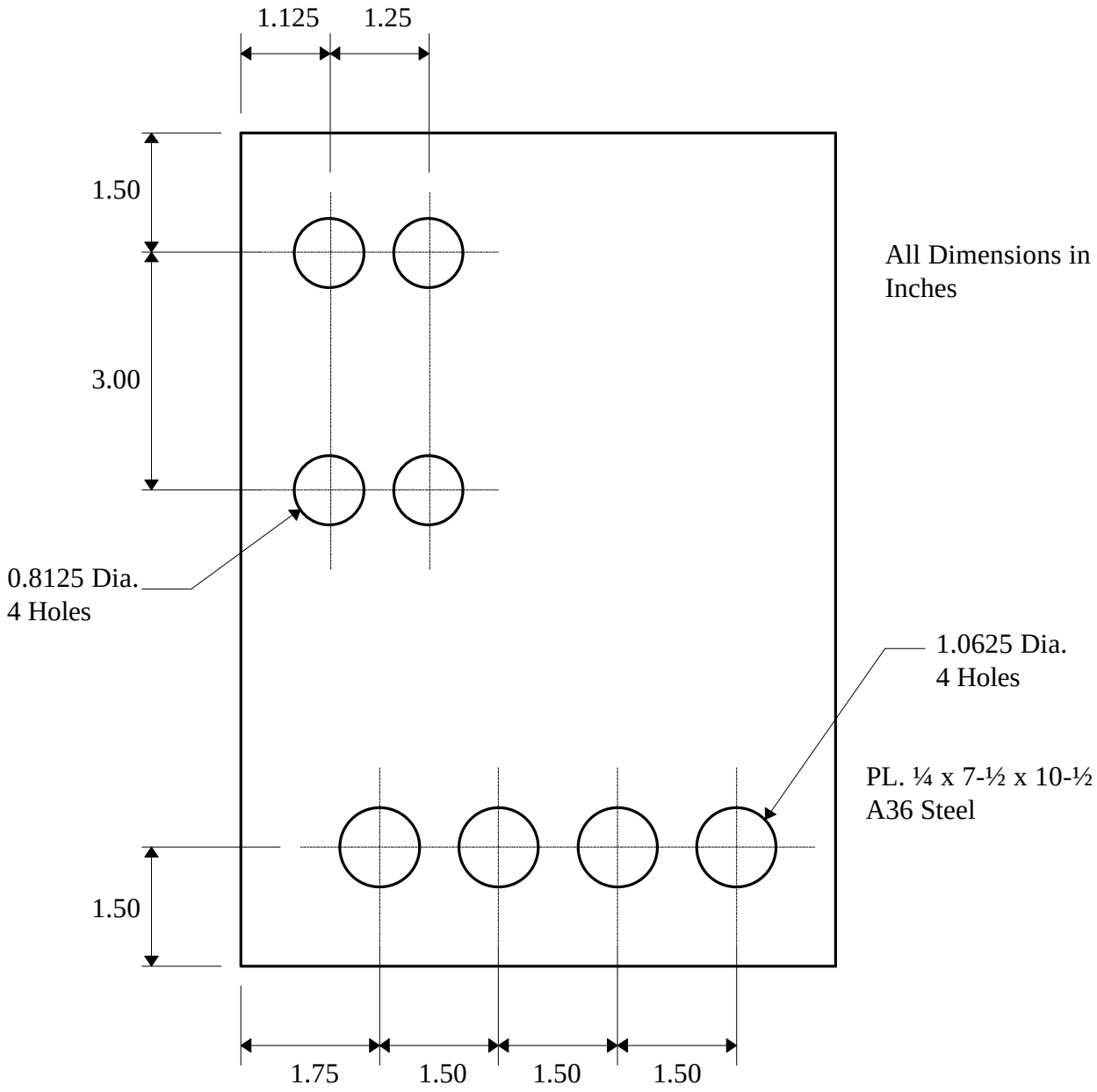

Figure 3.4 Dimensions of grip plate for the 2x4 test specimens.

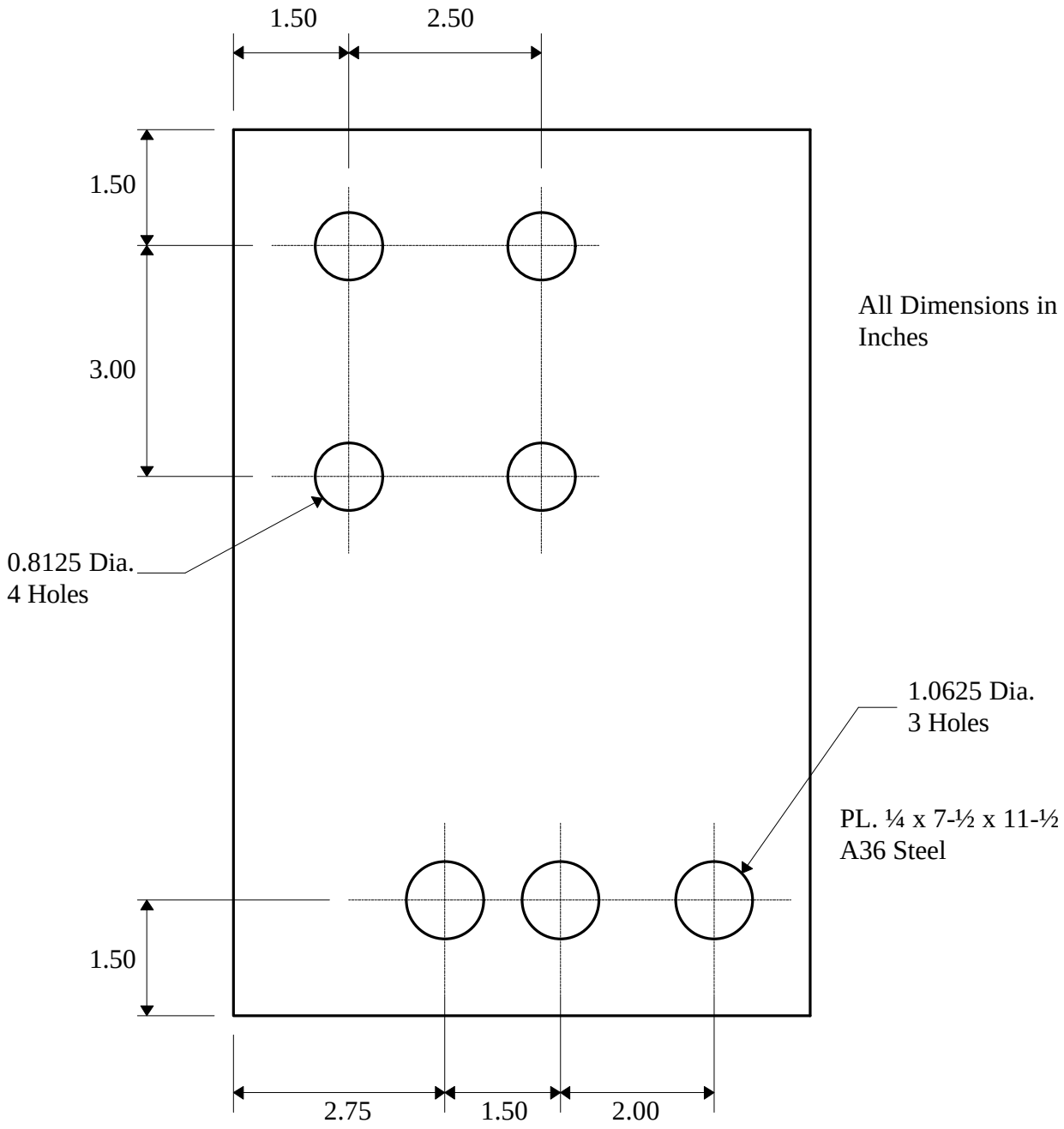

Figure 3.5 Dimensions of grip plate for the 2x6 test specimens.

The levels of eccentricity used for the 2x4 and 2x6 joints were chosen for several reasons. Economic constraints required that the total number of splice joints tested be kept to a minimum. The two previous studies of combined loading of splice joints were also considered. Gupta (1994) used eccentricities of 0.5, 1.0, 1.5, and 2.0 in. Wolfe (1990) used eccentricities of 0.875, 2.625, and 7.875 in. The smallest eccentricity possible with the grip plates used for this study was 1.5 in. because of the one-inch diameter holes needed for the steel pin that connected the grip plates to the testing machine. Thus, the eccentricities had to be in increments of 1.5 in. or more. In addition, the size (and thus weight) of the grip plates were kept to a minimum for ease of handling.

Three levels of eccentricity were selected for the 2x4 splice joints; 1.5, 3.0, and 4.5 in. Because two different gauges of truss plates were used for the 2x6 splice joints, only two levels of eccentricity were selected; 1.5, and 3.5 in. A large eccentricity, such as the 7.875 in. used by Wolfe, was not chosen because that would result in a very high moment relative to the tension, and most actual truss splice joints do not experience such loading conditions.

The grip plates had V-shaped grooves machined into the surfaces that contacted the lumber faces. These grooves were about $\frac{1}{8}$-in. deep and ran parallel to the length of the grip plates. The purpose of the grooves was to prevent failure in the lumber near the bolt holes due to perpendicular-to-grain tension stresses. Without the grooves, the grip plates would rotate slightly relative to the lumber when eccentric loads were applied, causing tension perpendicular-to-grain failures. Several of the test joints experienced such failures, and thus were discarded. When the grooves were added, the grip plates could be bolted on tightly, causing the grooves to press into the surface of the lumber and thereby preventing the grip plates from rotating.

3.2 Fabrication of Test Joints

To simulate actual splice joints in complete truss assemblies, the test joints were fabricated in much the same way as actual truss joints. A local wood truss manufacturer fabricated the test specimens using lumber from their stock. All lumber used was No. 2 KD19 Southern Pine. The 2x4 lumber was available in ten-foot lengths, and the 2x6 lumber was available in eight-foot lengths. The lumber was carefully selected to ensure that no knots would be located in the joint area.

Each eight-foot long 2x6 was sawn to fabricate two test specimens from the length of lumber, as shown in Figure 3.6. The first two quarter-lengths of the piece, labeled with the number one, were kept together and used to fabricate one test joint. The remaining two pieces were also kept together and used to make a second test joint. A one-inch wide block was cut from the middle of each four-foot half and placed in an airtight plastic bag. Later, this block was used to determine

the moisture content and specific gravity of the lumber used to make the test specimen. Moisture content was determined by the secondary oven-drying method of ASTM D4442 (ASTM, 1996c), and was based on oven-dry weight. Specific gravity was determined by the water immersion method of ASTM D2395 (ASTM, 1996d), and was based on oven-dry weight and oven-dry volume. The average values of specific gravity and moisture content of the lumber used for the test joints are given in Table 3.3.

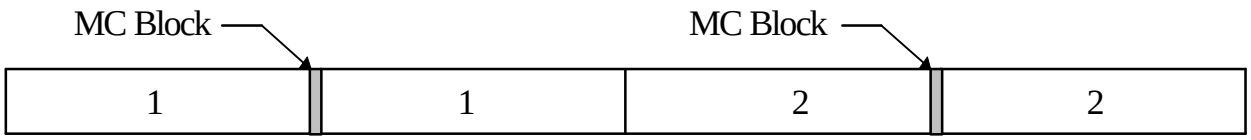

Figure 3.6 Assembly pattern for 2x6 test specimens.

Table 3.3 Average specific gravity (SG) and moisture content (MC) data for the lumber used for the joint tests.

Lumber Size	Plate Gauge	Number of Specimens[a]	Average SG[b]	COV[c] of SG (%)	Average MC[d] (%)	COV of MC (%)
2x4	20	24	0.55	15	15.0	21
2x6	20	18	0.56	12	13.6	20
2x6	16	15	0.56	14	16.5	23

[a]Total number of test specimens for all loading combinations
[b]Based on oven-dry weight and oven-dry volume
[c]Coefficient of variation
[d]Based on oven-dry weight

Two 2x4 test specimens were fabricated from each ten-foot length of 2x4 lumber by sawing the lumber as shown in Figure 3.7. The 2x4 lumber was available in ten-foot lengths, and the excess lumber was discarded. As with the 2x6 specimens, one-inch wide blocks were cut and later used for determining the moisture content and specific gravity of the lumber used to make the test joint.

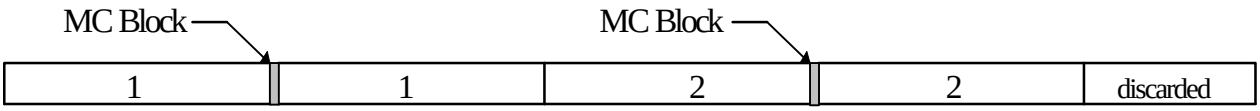

Figure 3.7 Assembly pattern for 2x4 test specimens.

After all of the lumber was cut, a matched pair of lengths were placed together and joined with a pair of truss plates. The two halves of the joint were butted closely together to form a joint with minimal gap between the two lumber halves. For most of the joints fabricated, the two halves were joined together in the same orientation in which they were cut from the full length of lumber. However, if they did not butt together very closely, they were rearranged so that the joint had a minimal gap. One truss plate was centered on the joint and tacked in place with a few light hammer taps along one lengthwise edge. Next, the joint was turned over, and another truss plate was centered on the joint and tacked at one corner. Finally the truss plates were pressed into the lumber using a hydraulic platen press. After pressing, each joint was checked to ensure that the truss plates were fully pressed into the lumber, but not over-pressed. In addition, both the average gap and maximum gap were checked to ensure that the TPI requirements for tension splice joint gaps were met. These requirements, given in Section 4.6.4 of ANSI/TPI 1-1995, state that immediately after fabrication, the maximum gap shall not exceed $\frac{1}{8}$ in. and the average gap shall not exceed $\frac{1}{16}$ in.

After fabrication, all test joints were stored in the testing laboratory for at least seven days at normal room temperature and relative humidity. The equilibrium moisture content of lumber depends on the environmental factors of dry-bulb temperature and relative humidity. The tooth withdrawal strength of truss plates is related to the moisture content of the lumber, but since the objective of these tests was to produce steel net-section failures and not tooth withdrawal failures, it was not necessary to store them in a lumber conditioning room at a certain temperature and relative humidity.

Each test joint was prepared for testing by trimming the length of each lumber half of the joint to 22 in., resulting in an overall specimen length of 44 in. Also, four $\frac{13}{16}$-in. diameter holes were drilled in each end of the joint to accommodate the bolts for the grip plates.

The overall specimen length of 44 in. was chosen for several reasons. First, this choice allowed two specimens to be fabricated from each eight-foot length of lumber. Second, this specimen

length was about the longest that could be tested on the testing machine used in this study. Finally, when testing splice joints in combined loading, Wolfe et al. (1991) advised that specimen length should be kept to a minimum to reduce the secondary moment effect caused by the transverse deflection of the specimen under the bending moment. This secondary moment effect (also called the P-Δ effect) reduces the load eccentricity and thus the moment at the joint, and is more pronounced for longer members. However, in this study, a linear variable differential transducer (LVDT) was used to measure the transverse deflection so that the actual eccentricity at failure could be determined by subtracting the transverse deflection at failure from the initial eccentricity.

3.3 Test Method

All test joints were loaded to failure using an MTS universal hydraulic testing machine. The 50,000-lb. capacity testing machine was connected to a data acquisition computer for recording load and displacement readings. A load cell attached to the hydraulic piston measured the applied tension force, and an LVDT measured the displacement of the piston.

For the tension-only tests, each specimen was attached to the MTS machine using the first hole on the grip plates. A tension load was applied using stroke (displacement) control. A displacement rate of 0.12 in./min was used, which resulted in failure times of 3 to 5 minutes. Six specimens were tested for each of the 2x4 lumber joints, as were six of the 20-gauge 2x6 joints. Only three specimens were tested for the 16-gauge 2x6 joints. Several test joints loaded in combined loading had wood failures in the bolted area due to tension-perpendicular-to-grain stresses. The addition of grooves on the surface of the grip plates (as described earlier) eliminated such failures; however, the number of remaining test joints would not allow the testing of six specimens for each loading level. Since the combined loading tests were of more interest than the tension-only tests, only three 16-gauge 2x6 joint specimens were tested in tension-only.

Before testing each combined loading specimen, the joint gap was measured on both sides of the joint. The two measurements were recorded as “compression gap” (i.e., the gap on the compression side of the joint) and “tension gap” (the gap on the tension side). When the grip plates were bolted to each specimen, the specimen was randomly oriented, so that the side of the joint with the larger gap may have been on the compression side or the tension side. The displacement rates for the combined loading tests varied for each of the combinations of initial eccentricity and joint configuration so that failures occurred in three to five minutes.

Figure 3.8 is a photograph of the test setup, showing a 2x6 splice joint failing under combined loading. The LVDT to the left of the test specimen measured the transverse deflection of the specimen.

Figure 3.7 Photograph of the test setup used to produce combined tension and bending stresses in the tested splice joints by applying an eccentric axial tension load.

4. Results

4.1 Tension-only Tests

Several splice joints of each of the three configurations of lumber size and plate gauge were loaded in tension-only to determine the ultimate strength of the steel net-section of the truss plates under direct tension stresses. All of the test results reported here for the splice joints tested in tension-only had failures in the steel net-section of the truss plates. Some of the test specimens with low specific gravities had failures in the lumber section near the bolts; each of those specimens was discarded and the test was repeated.

All of the joints failed in 3 to 5 minutes after the start of the test. Failure began as yielding of the steel plates at the gap, followed by the steel rupturing across the gap. Figure 4.1 shows typical failures for each of the three plate types tested.

The results of the tests of the 2x4 splice joints with 20-gauge plates loaded in tension-only are given in Table 4.1. An average ultimate tension strength of 11,979 lb. was observed. The coefficient of variation (COV) of the ultimate tension strength was very small (0.77%). Six replicates were tested; this is in accordance with the standard test method for steel net-section strength discussed earlier, given in ANSI/TPI 1-1995.

Table 4.2 gives the ultimate tension strengths for the 2x6 splice joints with 20-gauge truss plates. The average ultimate strength of the steel net-section was 19,454 lb., with a COV of 1.2%. As with the 2x4 joints, six replicates were tested.

The ultimate tension strengths of the 2x6 joints with 16-gauge plates are given in Table 4.3. Only three replicates were tested, as explained earlier in Section 3.3. The average ultimate tension strength of the 16-gauge plates was 23,633 lb., with a COV of 2.7%. The COV of the ultimate strength was again quite low.

Considering the very low COV's for all three of the joint configurations, testing fewer replicates when determining the ultimate steel net-section strength of truss plates would still give acceptable results in addition to being more economical than testing six replicates.

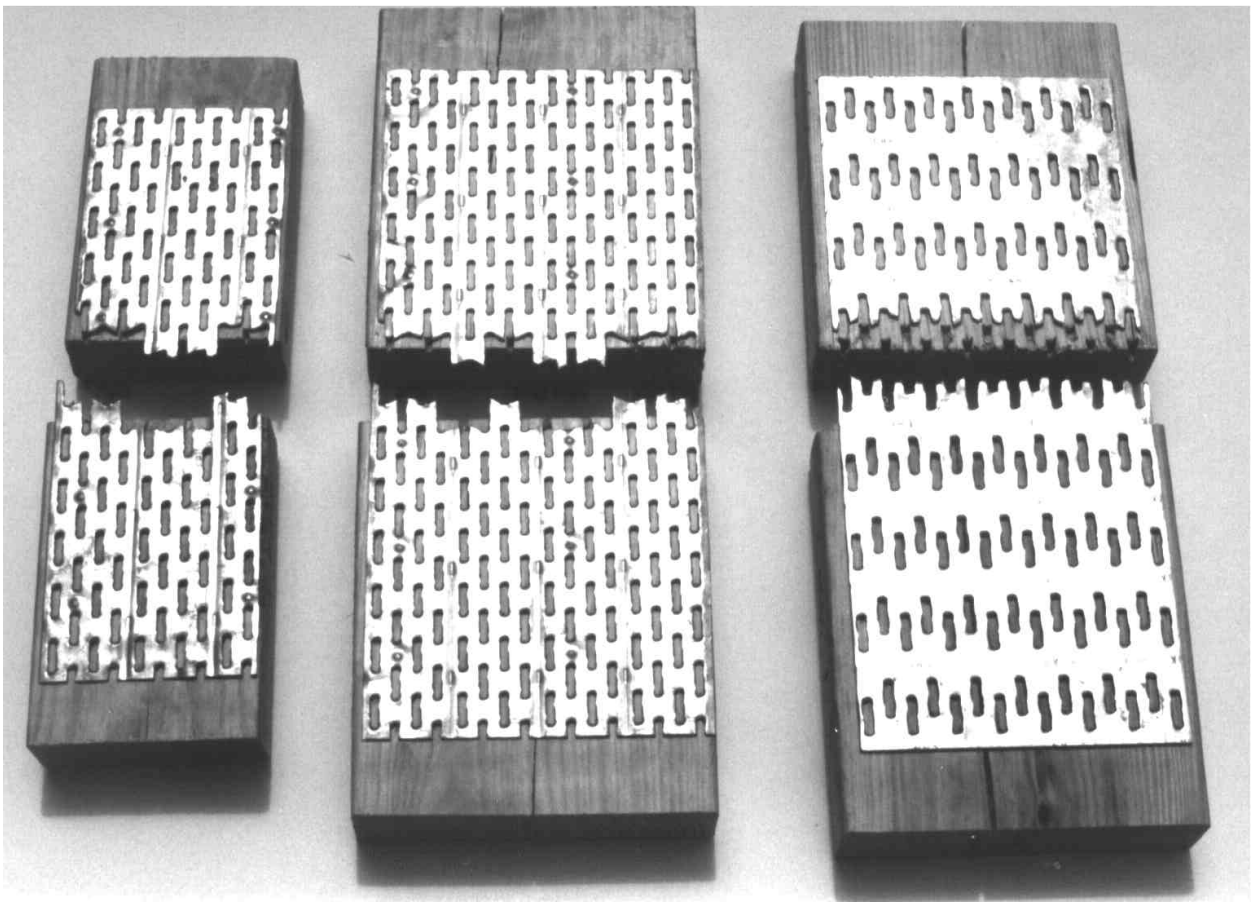

Figure 4.1 **Typical failures for the three joint configurations tested in tension-only loading. Shown in the photograph, from left to right, are a 2x4 joint with 20-gauge plates, a 2x6 joint with 20-gauge plates, and a 2x6 joint with 16-gauge plates.**

Table 4.1 Test results for 2x4 lumber, 20-gauge plates, tension-only loading.

Replicate Number	Tension Load at Failure (lb.)
1	11,987
2	12,109
3	11,841
4	12,012
5	12,012
6	11,914
Average	11,979
COV (%)	0.77

Table 4.2 Test results for 2x6 lumber, 20-gauge plates, tension-only loading.

Replicate Number	Tension Load at Failure (lb.)
1	19,678
2	19,336
3	19,605
4	19,067
5	19,580
6	19,458
Average	19,454
COV (%)	1.2

Table 4.3 Test results for 2x6 lumber, 16-gauge plates, tension-only loading.

Replicate Number	Tension Load at Failure (lb.)
1	24,316
2	23,511
3	23,071
Average	23,633
COV (%)	2.7

4.2 Combined Loading Tests of 2x4 Joints with 20-gauge Plates

The results of testing 2x4 joints with 1.5 in. of initial eccentricity are given in Table 4.4. Six replicates were tested. The transverse deflection, Δ, was measured by an LVDT attached to a fixed point on the test machine and to the center of the joint area. The moment at failure was calculated as:

$$M = T(e - \Delta) \qquad \text{(Eq. 4.1)}$$

where:

M is the calculated moment at failure,
T is the measured applied load,
e is the initial eccentricity, and
Δ is the transverse deflection at failure.

The average ultimate tension load was 7,967 lb., with a COV of 7.3%. This load represents about two-thirds of the ultimate tension-only capacity of 11,979 lb. for the truss plates. The average moment at the joint at failure was 6,777 in.-lb., with a COV of 6.7%.

The results of the tests of 2x4 joints with 3.0 in. of initial eccentricity are shown in Table 4.5. The moments at failure were calculated using Equation 4.1. Although six specimens were tested, only three replicates are reported. The deleted replicates had unreasonable LVDT readings for the transverse deflections, resulting from improper setup of the LVDT for each of the deleted tests. Unfortunately, this error was not realized until after all of the tests had been completed. The deleted tests could not be repeated because no truss plates remained from the same steel coil.

Extra test specimens were fabricated; however, they were used to replace the specimens that had failed at the bolts of the grip plates due to tension perpendicular-to-grain stresses.

The average ultimate tension load was 4,321 lb., representing about one-third of the ultimate tension-only capacity of the plates. The average moment at failure was 8,515 in.-lb., with a COV of 7.4%.

The coefficient of variation of the average ultimate load for the three replicates was 23%, considerably higher than the COV for the 2x4 joints with 1.5 in. of initial eccentricity. The moisture content of the first two test joints was about 15%. The third test joint, with an ultimate tension load of 5,469 lb., had a moisture content of nearly 20% at the time of fabrication and about 60% more transverse deflection than the other two tested joints. The additional transverse deflection for the third replicate allowed the joint to carry additional tensile load, and even more moment at failure. These results demonstrate the complex interaction of the tension, moment, and rotational stiffness of the joint. This may explain the relatively higher COV for these tests.

Table 4.6 shows the results of the test of 2x4 joints with 4.5 in. of initial eccentricity. Of the six replicates tested, three were deleted because of unreasonable LVDT readings. The average ultimate tension load was 2,995 lb., with a COV of 1.9%. This load is about one-quarter of the ultimate tension-only capacity of the plates. The average moment at failure was 10,645 in.-lb., with a COV of 5.3%.

All of the 2x4 joints with 20-gauge plates tested in the three levels of combined loading failed in the same manner. First, the gap on the compression side of the joint closed as the truss plates buckled locally over the gap on the compression side. This gap closure happened early during the test. The steel at the gap on the tension side began to yield, and then it began to rupture. Ultimate failure finally occurred as the steel continued to rupture across the tension side of the joint. All of these joints experienced both localized plate buckling and closure of the joint gap, followed by tension rupture of the plates. Figure 4.2 shows typical failures for the 2x4 joints loaded in combined loading.

Table 4.4 Test results for 2x4 lumber, 20-gauge plates, 1.5 in. initial eccentricity.

Replicate Number	Tension Gap (in.)	Compression Gap (in.)	Tension Load at Failure (lb.)	Transverse Deflection at Failure (in.)	Moment at Failure (in.-lb.)
1	0.045	0.006	8,252	0.7152	6,476
2	0.060	0.030	8,936	0.7267	6,910
3	0.034	0.030	7,837	0.5627	7,346
4	0.012	0.045	7,788	0.6104	6,928
5	0.016	0.006	7,202	0.5342	6,956
6	0.010	0.000	7,788	0.7238	6,045
Average			7,967	0.6455	6,777
COV (%)			7.3	14	6.7

Table 4.5 Test results for 2x4 lumber, 20-gauge plates, 3.0 in. initial eccentricity.

Replicate Number	Tension Gap (in.)	Compression Gap (in.)	Tension Load at Failure (lb.)	Transverse Deflection at Failure (in.)	Moment at Failure (in.-lb.)
1	0.010	0.045	3,784	0.7956	8,341
2	0.000	0.065	3,711	0.8459	7,992
3	0.019	0.008	5,469	1.3155	9,213
Average			4,321	0.9857	8,515
COV (%)			23	29	7.4

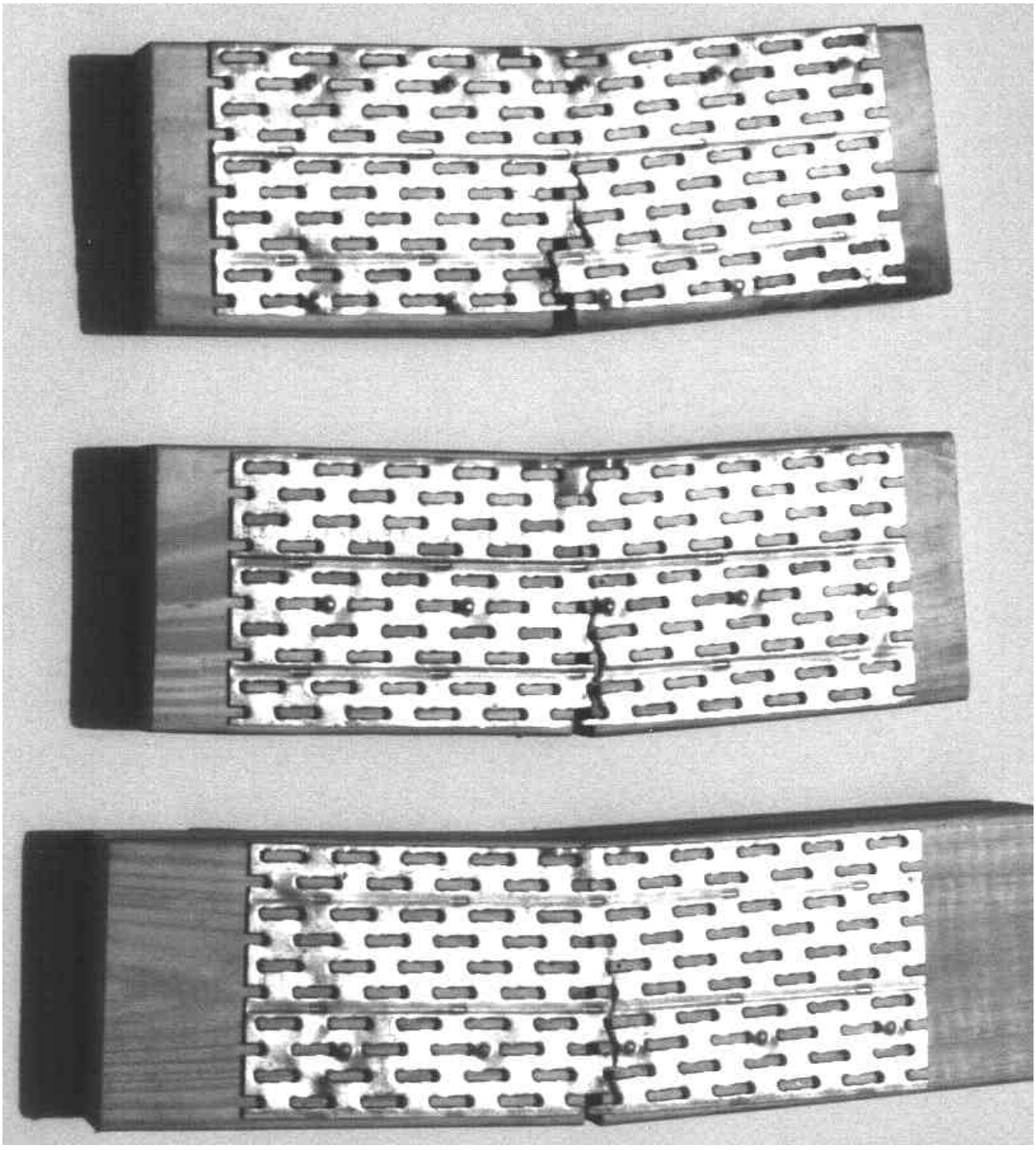

Figure 4.2 Typical failures for the 2x4 joints tested in combined tension and bending loading.

Table 4.6 Test results for 2x4 lumber, 20-gauge plates, 4.5 in. initial eccentricity.

Replicate Number	Tension Gap (in.)	Compression Gap (in.)	Tension Load at Failure (lb.)	Transverse Deflection at Failure (in.)	Moment at Failure (in.-lb.)
1	0.040	0.025	2,930	1.0814	10,016
2	0.010	0.000	3,027	0.8373	11,087
3	0.008	0.016	3,027	0.9220	10,831
Average			2,995	0.9469	10,645
COV (%)			1.9	13	5.3

4.3 Combined Loading Tests of 2x6 Joints with 20-gauge Plates

The results of testing 2x6 splice joints with 20-gauge plates and 1.5 in. of initial eccentricity are given in Table 4.7. Four replicates are reported; two of the six joints tested had unreasonable LVDT readings and thus were deleted because the actual moment at failure could not be determined. The average ultimate tension load was 13,080 lb., representing about two-thirds of the ultimate tension-only capacity (19,454 lb.) of the truss plates used for these joints. The average moment at failure was 14,899 in.-lb.

Table 4.8 gives the results of the tests of 2x6 joints with 20-gauge plates and 3.5 in. of initial eccentricity. An average ultimate tension load of 7,153 lb. was observed. This load is about one-third of the ultimate tension-only capacity of the plates. The average moment at failure was 21,575 in.-lb.

The COV's of the ultimate tension and moment for both of the combined loading levels of the 2x6 joints with 20-gauge plates are very low, about 4%. This indicates that testing fewer replicates can still give consistent results.

The 2x6 joints with 20-gauge plates all failed in essentially the same manner as the 2x4 joints with 20-gauge plates. The compression gap closed as the plates buckled, resulting in wood-to-wood contact on the compression side. The steel on the tension side began to yield, then finally ruptured as the ultimate load was reached. Figure 4.3 shows typical failures.

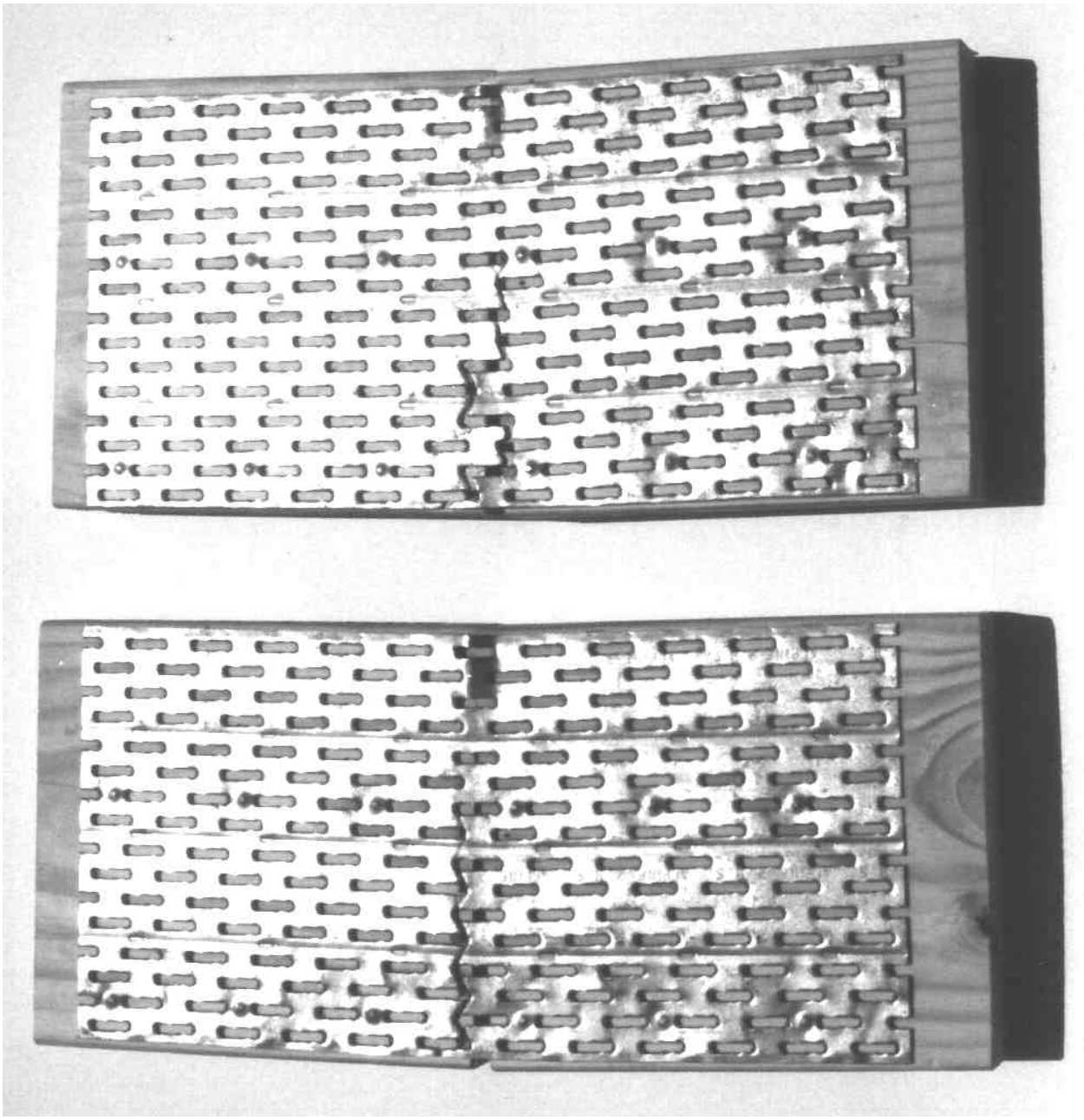

Figure 4.3 **Typical failures for the 2x6 joints with 20-gauge plates tested in combined tension and bending loading.**

Table 4.7 Test results for 2x6 lumber, 20-gauge plates, 1.5 in. initial eccentricity.

Replicate Number	Tension Gap (in.)	Compression Gap (in.)	Tension Load at Failure (lb.)	Transverse Deflection at Failure (in.)	Moment at Failure (in.-lb.)
1	0.006	0.008	13,574	0.3562	15,526
2	0.006	0.016	12,940	0.3404	15,005
3	0.012	0.006	12,769	0.3475	14,716
4	0.035	0.006	13,037	0.3993	14,350
Average			13,080	0.3609	14,899
COV (%)			2.7	7.3	3.3

Table 4.8 Test results for 2x6 lumber, 20-gauge plates, 3.5 in. initial eccentricity.

Replicate Number	Tension Gap (in.)	Compression Gap (in.)	Tension Load at Failure (lb.)	Transverse Deflection at Failure (in.)	Moment at Failure (in.-lb.)
1	0.006	0.025	6,714	0.4998	20,143
2	0.020	0.020	7,324	0.4581	22,279
3	0.012	0.014	7,129	0.4251	21,921
4	0.006	0.006	7,446	0.5515	21,955
Average			7,153	0.4836	21,575
COV (%)			4.5	11	4.5

4.4 Combined Loading Tests of 2x6 Joints with 16-gauge Plates

Table 4.9 lists the results of testing 2x6 joints with 16-gauge plates and 1.5 in. of initial eccentricity. The average ultimate tension load was 15,601 lb. This load is about two-thirds of the ultimate tension-only capacity of the plates. The average moment at failure was 15,774 in.-lb.

The results of testing 2x6 joints with 16-gauge plates and 3.5 in. of initial eccentricity are given in Table 4.10. An average tension load of 9,434 lb. was observed, representing about two-fifths of the ultimate tension-only capacity of the plates. The average moment at failure was 26,518 in.-lb. Five replicates were reported, since one test joint had unreasonable LVDT readings. Again, the COV's of the average tension and moment were low.

The failures for these joints with 16-gauge plates were similar to the failures for the 20-gauge plates, except that the 16-gauge plates generally did not buckle. However, the gap on the compression side did close for all of the joints tested. Figure 4.4 shows typical failures for these joints.

Table 4.9 Test results for 2x6 lumber, 16-gauge plates, 1.5 in. initial eccentricity.

Replicate Number	Tension Gap (in.)	Compression Gap (in.)	Tension Load at Failure (lb.)	Transverse Deflection at Failure (in.)	Moment at Failure (in.-lb.)
1	0.012	0.008	16,235	0.5501	15,422
2	0.010	0.010	14,868	0.4423	15,726
3	0.026	0.025	16,357	0.4854	16,596
4	0.030	0.045	15,772	0.4955	15,843
5	0.010	0.008	14,673	0.4366	15,603
6	0.035	0.022	15,698	0.5156	15,453
Average			15,601	0.4876	15,774
COV (%)			4.4	8.9	2.7

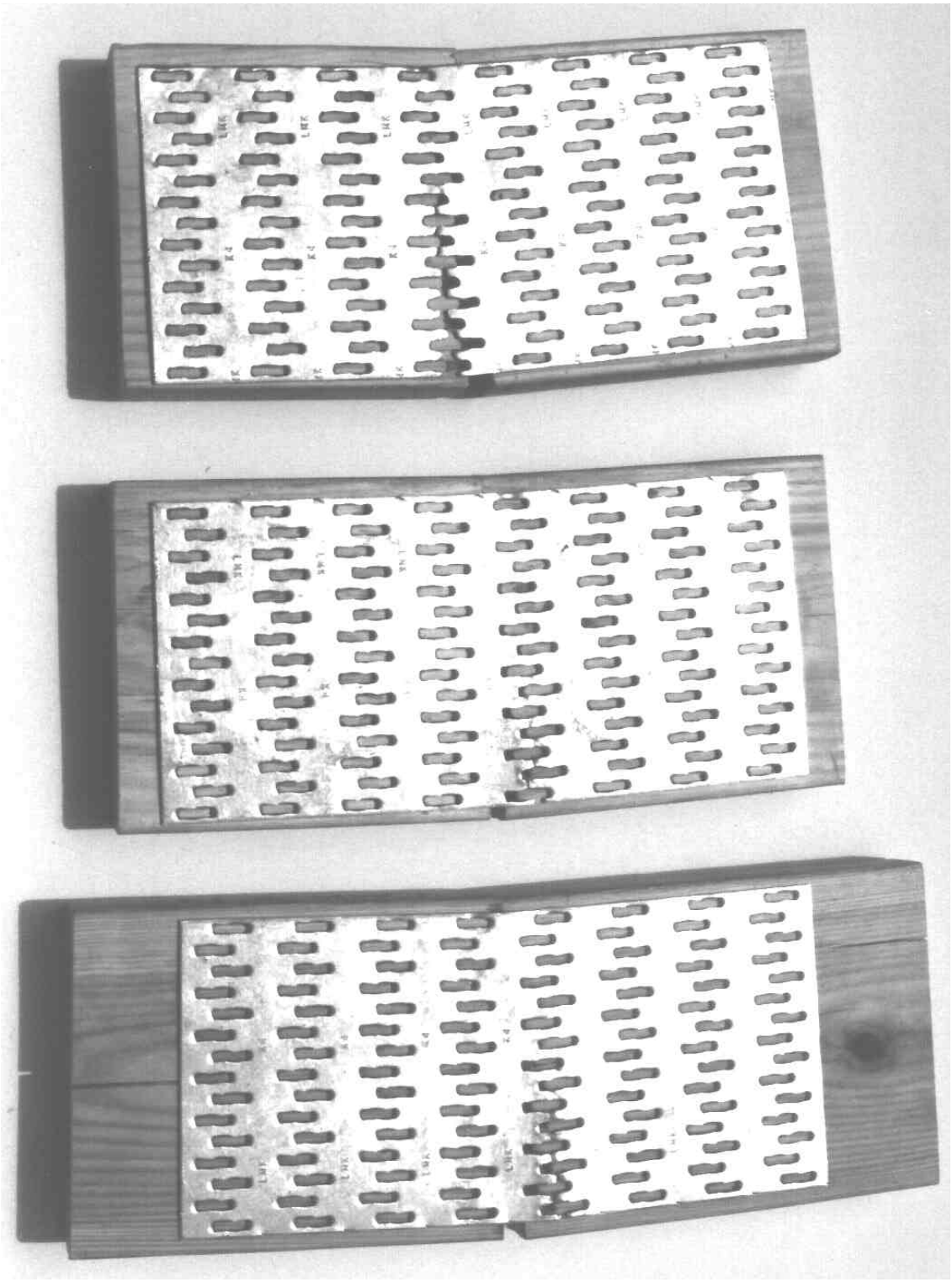

Figure 4.4 Typical failures for the 2x6 joints with 16-gauge plates tested in combined tension and bending loading.

Table 4.10 Test results for 2x6 lumber, 16-gauge plates, 3.5 in. initial eccentricity.

Replicate Number	Tension Gap (in.)	Compression Gap (in.)	Tension Load at Failure (lb.)	Transverse Deflection at Failure (in.)	Moment at Failure (in.-lb.)
1	0.030	0.012	9,473	0.6190	27,300
2	0.026	0.010	9,668	0.7454	26,631
3	0.034	0.026	9,424	0.6362	26,988
4	0.030	0.025	9,644	0.7870	26,164
5	0.025	0.025	8,960	0.6534	25,506
Average			9,434	0.6882	26,518
COV (%)			3.0	11	2.7

4.5 Relationship Between Joint Gap and Ultimate Moment

To determine if a relationship exists between the average gap at a splice joint prior to testing and the ultimate moment (i.e., the moment at failure), a regression analysis was conducted. For each of the three joint configurations, the correlation between the average gap and the standardized ultimate moment was investigated. The ultimate moment was standardized so that all of the levels of combined loading could be compared for each of the three plate types used and have an equal weight in the statistical analysis. Equation 4.2 shows how the ultimate moment was standardized for the 2x4 joints:

$$m_{i,e} = \frac{M_{i,e} - \overline{M}_e}{s_e} \qquad (4.2)$$

where:

- $m_{i,e}$ is the standardized moment at failure for the i^{th} replicate of the tests of the 2x4 joints with 20-gauge plates and e inches of initial eccentricity,
- $M_{i,e}$ is the ultimate moment at failure for the i^{th} replicate,
- $\overline{M}_e$ is the average ultimate moment at failure for the 2x4 joints with 20-gauge plates and e inches of initial eccentricity, and
- s_e is the standard deviation of the ultimate moment at failure for the 2x4 joints with 20-gauge plates and e inches of initial eccentricity.

Equation 4.2 was used to calculate the standardized ultimate moment for each level of eccentricity (1.5, 3.0, and 4.5 in.) for the 2x4 joints.

Next, using the average gap and the standardized moment for each of the 2x4 specimens tested in all levels of combined loading, a least squares regression analysis was conducted using a commercial statistical software package (Minitab, 1995). This statistical procedure tests the hypothesis that the response variable (in this case, the standardized ultimate moment) is related to the predictor variable (the average joint gap). The procedure fits a straight line to the data pairs. If the slope of the fitted line is close enough to zero, then it is concluded that the ultimate moment is not dependent on the average gap. The statistical procedure gives a result, called the p-value, which can be compared to a predetermined significance level called the α-level. If the p-value is greater than the chosen α-level, then the hypothesis of no relationship between the variables is not rejected, meaning that the ultimate moment does not depend on the gap. Typical p-values range from 0.01 to 0.1. Thus, a p-value larger than 0.1 would indicate that the hypothesis of no relationship is true, and thus the ultimate moment does not depend on the joint gap for the joints tested in this study. It should be noted that the joints tested in this study had gaps that ranged from 0.005 to 0.045 in. The maximum gap of 0.045 in. is 36% of the maximum gap allowed for a tension splice joint (ANSI/TPI 1-1995).

For the 2x4 joints with 20-gauge plates loaded in combined loading, the regression analysis gave a p-value of 0.904, indicating that the joint gap and the ultimate moment are not related. Figure 4.5 shows the regression line for the relationship between the standardized ultimate moment and the joint gap. The nearly horizontal line indicates that there is no relationship between moment and gap for the 2x4 joints.

The same regression analysis was done for the 2x6 joints. For the 2x6 joints with 20-gauge plates, the p-value from the analysis was 0.264. This suggests little evidence that the ultimate moment increases or decreases as a function of joint gap. Figure 4.6 also suggests that no significant relationship exists between the ultimate moment and joint gap for the 2x6 joints with 20-gauge plates.

The regression analysis for the 2x6 splice joints with 16-gauge plates gave a p-value of 0.577. Thus, ultimate moment and joint gap for these joints are not related. The regression line shown in Figure 4.7 supports this conclusion.

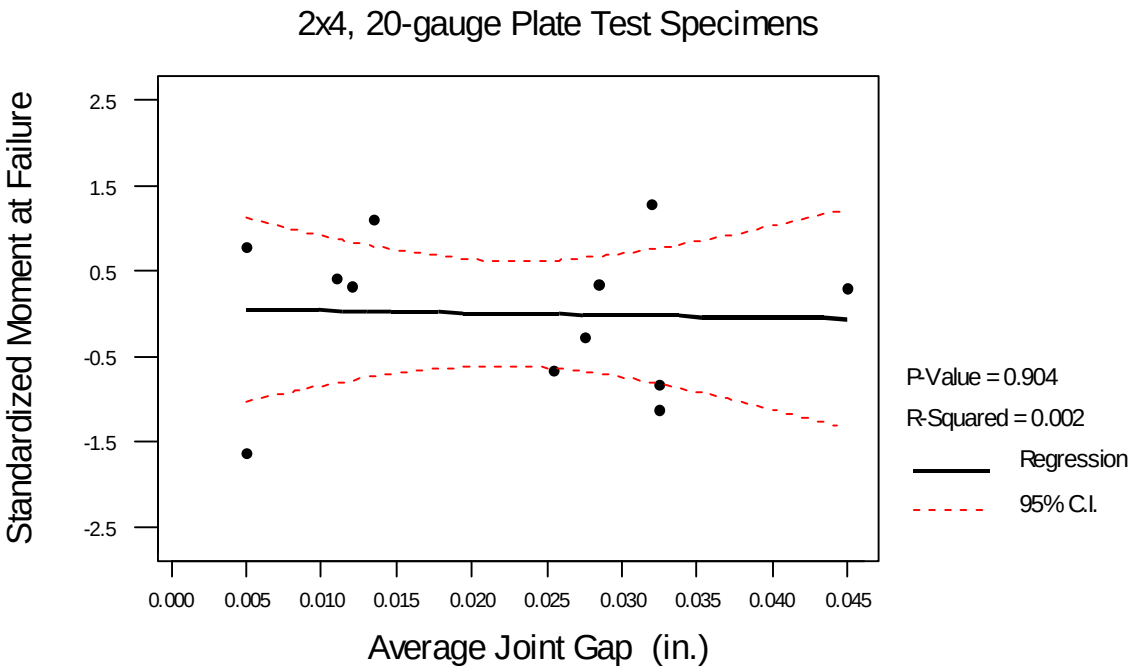

Figure 4.5 Relationship between standardized moment at failure and joint gap for 2x4 joints with 20-gauge plates.

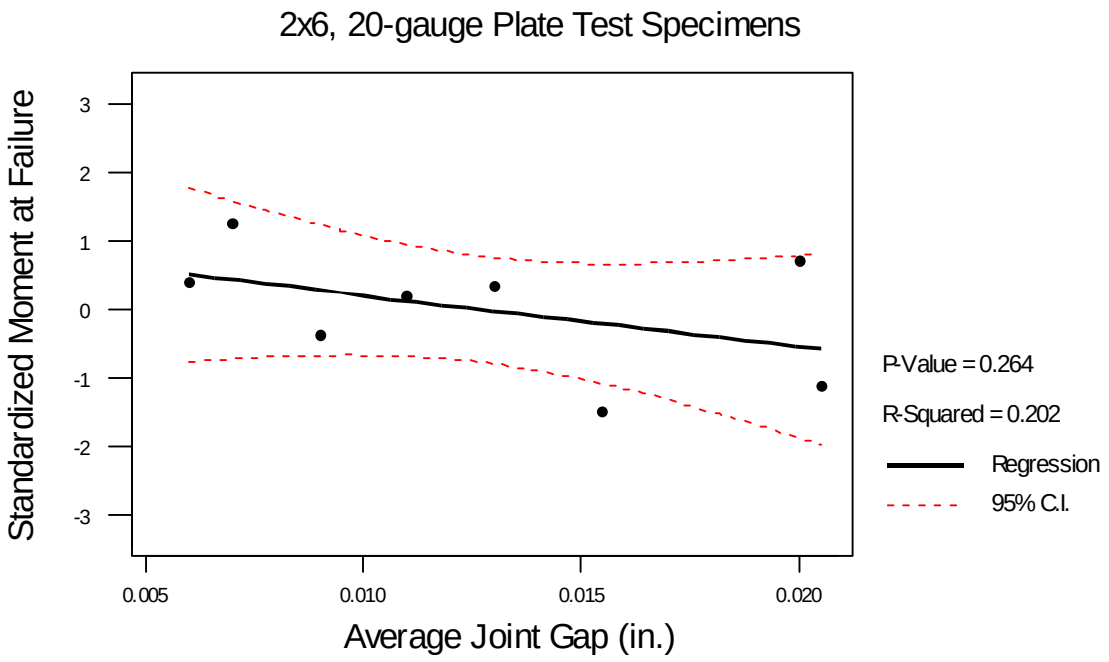

Figure 4.6 Relationship between standardized moment at failure and joint gap for 2x6 joints with 20-gauge plates.

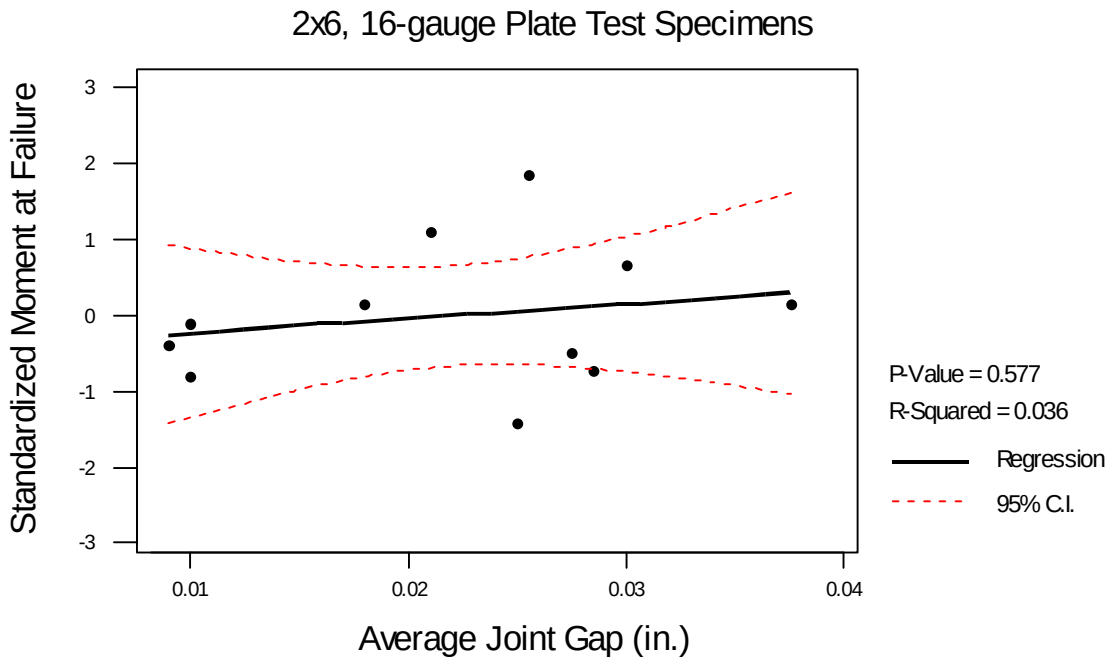

Figure 4.7 Relationship between standardized moment at failure and joint gap for 2x6 joints with 16-gauge plates.

5. Model Development

Three models were developed for predicting the ultimate moment capacity of the steel net-section of splice joints subjected to bending and tension. The data from the laboratory tests conducted for this study were used to evaluate the models. In addition, data from previous studies of combined loading of splice joints were used in the model evaluations. Finally, the most accurate model was selected, and a design method based on this model was developed.

5.1 Linear Stress Model (Model 1)

The three models presented are adaptations of three of Noguchi's (1980) models. The first model presented, Model 1, is similar to Noguchi's first model. Noguchi studied the steel net-section strength of splice joints in bending, and was only concerned with splice joints that had truss plates located below the neutral axis of the truss chord. Figure 5.1 shows a diagram of the splice joints Noguchi studied. When subjected to a bending moment, the wood-to-wood area contact carries the compressive component of the bending moment, and the steel truss plate carries the tensile component.

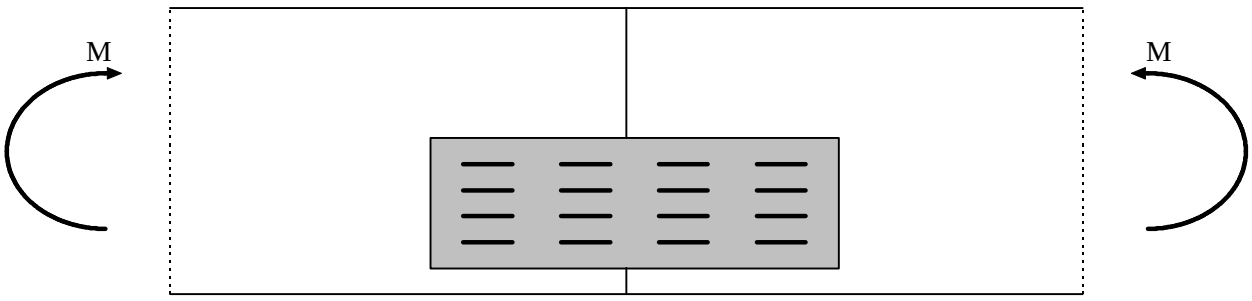

Figure 5.1 Splice joint studied by Noguchi (1980).

The first model Noguchi discussed was an elastic model, in which both the wood in compression and the steel in tension behave elastically. Figure 5.2 shows the assumed stress distribution for the splice joint shown in Figure 5.1. The neutral axis is not at the centerline of the truss chord because of the stress and cross-sectional area differences between the wood and the steel.

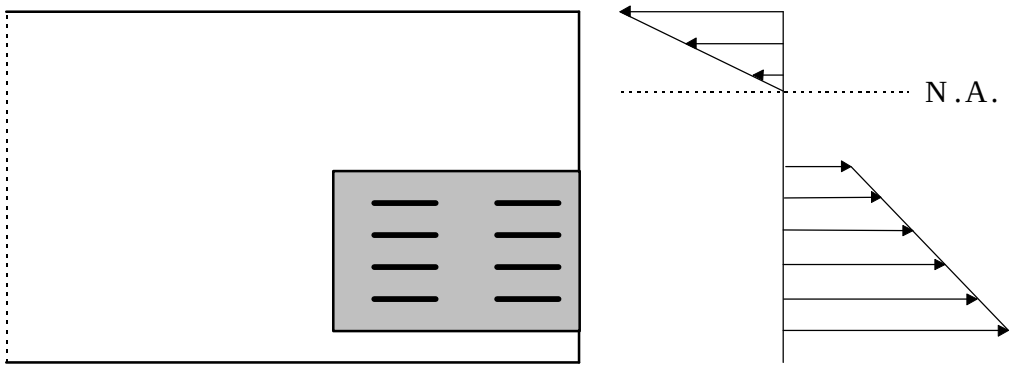

Figure 5.2 Elastic stress distribution for Noguchi s (1980) splice joint.

A similar model can be applied to splice joints with truss plates centered on the wide face of the lumber and subjected to tension and bending, such as those tested in this study. This model, Model 1, is based on a linear, but not elastic, stress distribution. Noguchi's first model was an elastic model; the maximum stress in the steel plate (at the bottom edge of the plates) was assumed to equal the elastic yield stress limit of the steel. Also, the maximum stress in the wood (at the top edge of the chord) was assumed to equal a theoretical elastic stress limit of the wood. In the model presented here, the maximum stress in the steel is assumed equal to the ultimate tensile stress of the truss plates, and the maximum stress in the wood is assumed to equal the ultimate compressive stress of the wood.

Figure 5.3 shows a free-body diagram of a splice joint for the combined loading tests of this study. Figure 5.4 shows one-half of the splice joint with the tension and moment caused by the eccentrically applied tension load. Figure 5.5 shows the assumed linear stress distribution for Model 1.

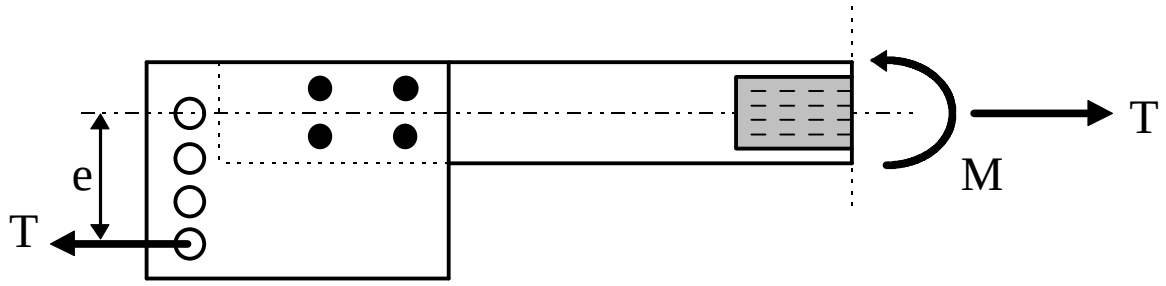

Figure 5.3 Free-body diagram of a splice joint.

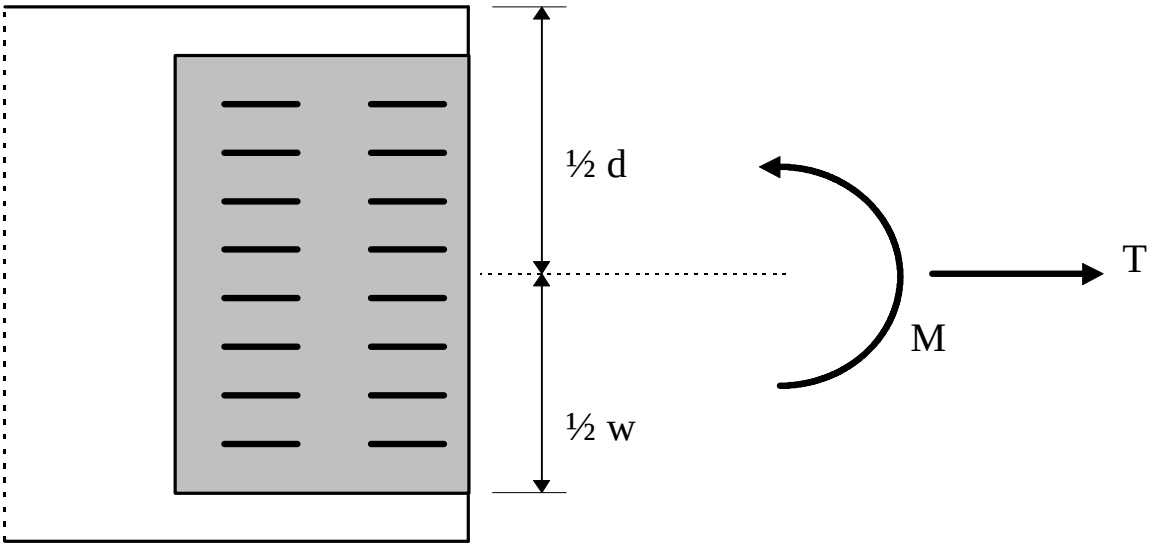

Figure 5.4 Tension and moment at splice joint caused by eccentrically applied load. The truss plate width is w, and d is the chord depth.

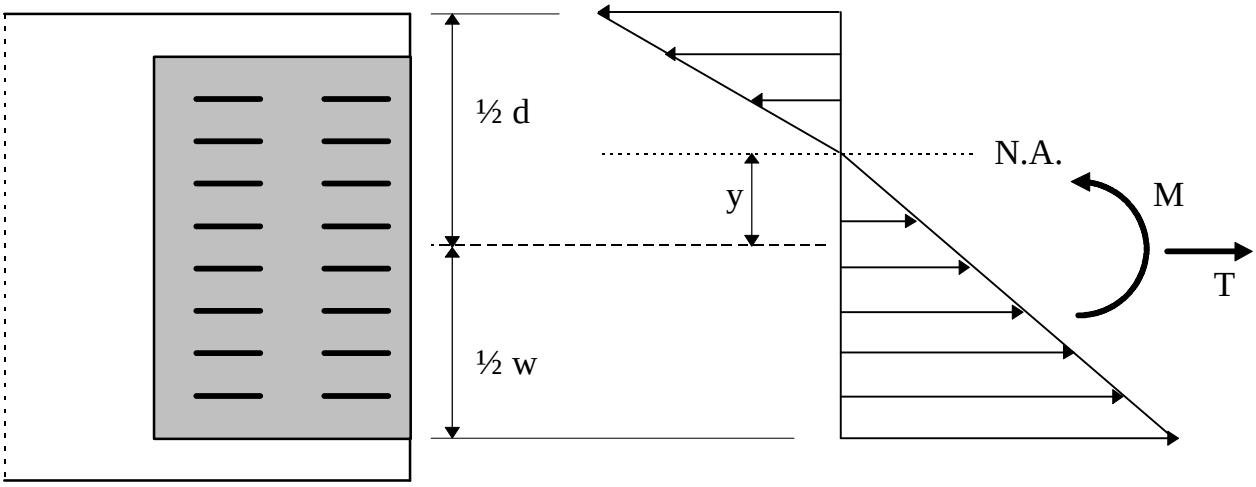

Figure 5.5 Assumed linear stress distribution for Model 1. The location of the neutral axis is y in. above the centerline of the truss chord.

In Figure 5.5, the neutral axis is not located at the centerline of the truss chord because of the different stresses in the wood and steel. The neutral axis is located a distance of y above the centerline of the truss chord. The top triangle represents the compressive stress in the wood, and the bottom triangle represents the tensile stress in the steel. In this model, the strength of the steel truss plates in compression is ignored, and wood-to-wood contact on the compression side of the joint is assumed. In all of the joints tested in combined loading, the gap on the compression side of the joint closed, causing wood-to-wood contact. Compression gap closure was caused by plate buckling for the 20-gauge truss plates, and by slippage between the plate teeth and the wood for the 16-gauge plates.

The assumptions for Model 1 are summarized below:

- The joint gap on the compression side of the joint closes and permits wood-to-wood contact.
- The compressive forces developed in the steel plates are negligible due to gap closure and consequent wood-to-wood bearing.
- The stress distributions for the wood and the steel are linear.
- The neutral axis is located within the truss plate.
- The wood and the steel both reach their maximum stresses, equal to their respective ultimate stresses, at the same time.

- The planes of the cross-sections of the steel in tension and the wood in compression each remain plane when subjected to bending.

The last assumption may not be a realistic assumption. Noguchi's first model was based on the similar assumption that the steel and wood reach their elastic limit simultaneously. These assumptions do not ensure strain compatibility; that is, that the strain rate of the steel and the strain rate of the wood are equal. If strain compatibility were ensured, then either the wood or the steel would reach its maximum stress first, and then the other would be at a stress level less than its maximum stress.

Figure 5.6 shows the stress distribution again, with the equivalent forces for the stresses in the wood and the steel. The equivalent forces F_{wood} and F_{steel} are shown in the opposite direction of the stress blocks because they represent the capacity or resistance of the joint to the applied loads T and M.

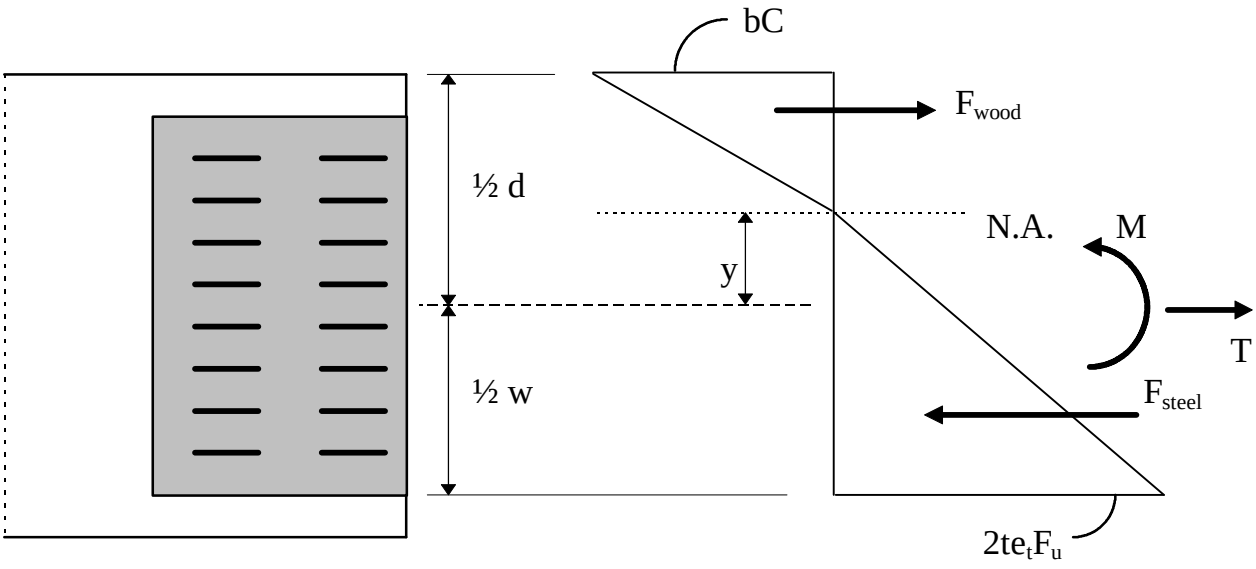

Figure 5.6 Stress distribution for Model 1. The forces F_{wood} and F_{steel} represent the resistance of the wood and the steel to the applied loads M and T.

The notation used in Figure 5.6 is explained below:

T is the applied axial force,
M is the applied moment,
F_{wood} is the compressive resistive strength of the wood under compression,
F_{steel} is the tensile resistive strength of the steel in tension,
N.A. is the neutral axis,
y is the distance from the chord centerline to the neutral axis,
F_u is the ultimate tensile strength of the truss plate steel,
e_t is the tension efficiency ratio for the truss plates,
C is the ultimate compressive strength of the wood,
d is the depth of the truss chord,
b is the thickness of the truss chord,
w is the width of the truss plate, and
t is the thickness of the truss plate.

The tension efficiency ratio, e_t, is the ratio of the ultimate tensile strength of a punched truss plate with a given width to the ultimate tensile strength of a solid plate with the same width and from the same steel coil. This ratio accounts for the reduction in strength as affected by the tooth pattern of the truss plate, the reduction of the cross-sectional area of the plate, the strain-hardening of the steel caused by the punching process, and the stress concentrations around the punched holes in the plate. Each truss plate configuration has a unique efficiency ratio that is determined from tests of the truss plate and a solid metal control specimen. The efficiency ratio for a particular truss plate can be found in a building code evaluation report for that truss plate.

The location of the neutral axis with respect to the centerline can be found by summing the forces, resulting in Equation 5.1:

$$(\sum F = 0) \qquad \tfrac{1}{2} * 2te_t F_u (\tfrac{1}{2} w + y) = \tfrac{1}{2} bC(\tfrac{1}{2} d - y) + T$$

$$y = \frac{\tfrac{1}{4} bdC + T - \tfrac{1}{2} twe_t F_u}{te_t F_u + \tfrac{1}{2} bC} \qquad (5.1)$$

Next, summing moments about the neutral axis results in Equation 5.2:

$$(\sum M = 0) \qquad M + Ty = \tfrac{1}{2} * 2te_t F_u (\tfrac{1}{2} w + y)^2 * \tfrac{2}{3} + \tfrac{1}{2} bC(\tfrac{1}{2} d - y)^2 * \tfrac{2}{3}$$

$$M + Ty = \tfrac{2}{3} te_t F_u (\tfrac{1}{2} w + y)^2 + \tfrac{1}{3} bC(\tfrac{1}{2} d - y)^2 \qquad (5.2)$$

These two equations can be solved simultaneously to find the maximum moment that can be applied in addition to the specified tension force at failure. The data collected in the tests of the actual splice joints were used in these equations to predict the moment, M, at joint failure. The actual applied tension force was used in the equations to solve for M, the predicted moment, and y, the location of the neutral axis. Then the predicted moment was compared to the actual applied moment. For each test group, the average values of the applied moment and tension force were used.

The values used for F_u, the ultimate tensile stress of the steel, were calculated using the average ultimate tensile strength for each type of truss plate, determined from the tension-only tests. Equation 5.3 shows how these values were calculated:

$$F_u = \frac{T}{2twe_t} \tag{5.3}$$

where:

F_u is the average ultimate tensile stress for the truss plate steel,
T is the average ultimate tension force for the given truss plate type,
t is the thickness of the truss plate,
w is the width of the truss plate, and
e_t is the tension efficiency ratio for the truss plates.

Table 5.1 shows these values for the three types of truss plates used in this study. Note that the average ultimate tensile stress determined from the tension-only tests for the 2x6 16-gauge splice joints was 69.5 ksi, considerably higher than the nominal ultimate stress for that grade of steel, 52 ksi. The higher stress determined from the tension-only tests was in part due to the positioning of a solid section of the plates over the joint in these tests, as illustrated in Figure 4.1.

The ultimate compressive strength of the wood, C, used in the equations was the average compressive strength for the grade and species of lumber used (No. 2 KD19 Southern Pine). This value, 4,139 psi, was taken from a summary of mechanical properties of visually graded lumber (Green and Evans, 1987). This value is the median of the ultimate compressive strength for 2x4 No. 2 Southern Pine at a 15% moisture content. No values were given for 2x6 lumber, so the same value was used for both the 2x4 and 2x6 joints.

The efficiency ratios used for the plates are given in Table 5.1. The plate dimensions used were taken from the descriptions of the truss plates given earlier in Table 3.1. All of this information about the truss plates was found in the building code evaluation report SBCCI PST & ESI Evaluation Report No. 94168 (SBCCI PST & ESI, 1995).

Table 5.1 Average ultimate tensile stress of the truss plate steel for each of the three types of plates used, as calculated from the tension-only joint tests.

Plate	Steel Grade	Gauge	Tension Efficiency Ratio[c], e_t	Joint Size	Average Ultimate Tension (lb.)	Average Ultimate Tensile Stress[d] (ksi)
Alpine HS2510	60[a]	20	0.71	2x4	11,979	72.2 (70)
Alpine HS412	60	20	0.71	2x6	19,454	73.3 (70)
Lumbermate K510	37[b]	16	0.591	2x6	23,633	69.5 (52)

[a]ASTM A653 HSLA Grade 60 steel.
[b]ASTM A653 SQ Grade 37 steel.
[c]Efficiency ratios are taken from SBCCI PST & ESI Evaluation Report No. 94168 (1995).
[d]The nominal ultimate tensile strength is given in parentheses.

Table 5.2 shows the predicted ultimate moment and the ratio of the predicted ultimate moment to the actual ultimate moment for each test group. If the model predicted the ultimate moment accurately, then the ratio of predicted to actual moment would be very close to one. As shown by the ratios of predicted to actual moment given in the table, this model does not fit the test data. For the lowest level of initial eccentricity (1.5 in. for each truss plate type), the neutral axis is located above the top edge of the truss plate. (For example, the value of y for the 2x4 joints with 1.5 in. of initial eccentricity is 2.111 in. Since the half of the truss plate width is 1.64 in., the neutral axis is located above the top edge of the plate.) For these cases, the model is inappropriate because the assumption that the neutral axis lies in the truss plate is violated. For the other cases, the model predicts an ultimate moment that is about sixty percent of the actual ultimate moment. The major inaccuracy of this model is a result of assuming that the stress distribution of the steel is linear.

Table 5.2 Predicted ultimate moments using Model 1 depicted in Figure 5.6.

Test Group Description[a]	Number of Tests	T_{actual}[b] (lb.)	M_{actual}[b] (in.-lb.)	$M_{predicted}$ (in.-lb.)	$M_{predicted}/M_{actual}$	y (in.)
2x4, 20-G, 1.5	6	7,967	6,777	575	0.085	*2.111*[c]
2x4, 20-G, 3.0	3	4,321	8,515	5,408	0.635	1.371
2x4, 20-G, 4.5	3	2,995	10,645	6,720	0.631	1.102
2x6, 20-G, 1.5	4	13,080	14,899	1,149	0.077	*3.380*
2x6, 20-G, 3.5	4	7,153	21,575	13,606	0.631	2.180
2x6, 16-G, 1.5	6	15,601	15,774	2,290	0.145	*3.336*
2x6, 16-G, 3.5	5	9,434	26,518	14,676	0.577	2.207

[a]Lumber size, plate gauge, and level of initial eccentricity (in.).
[b]The actual tension and moment values given are the averages for each test group.
[c]The italicized cells indicate that y, the estimated location of the neutral axis with respect to the centerline of the member, is above the top edge of the truss plate, and thus violates the assumptions of the model.

5.2 Plastic-Linear Stress Model (Model 2)

This model is similar to Noguchi's third model, which was based on plastic behavior for the steel and elastic behavior for the wood. The stress distribution for Noguchi's plastic-elastic model is shown in Figure 5.7.

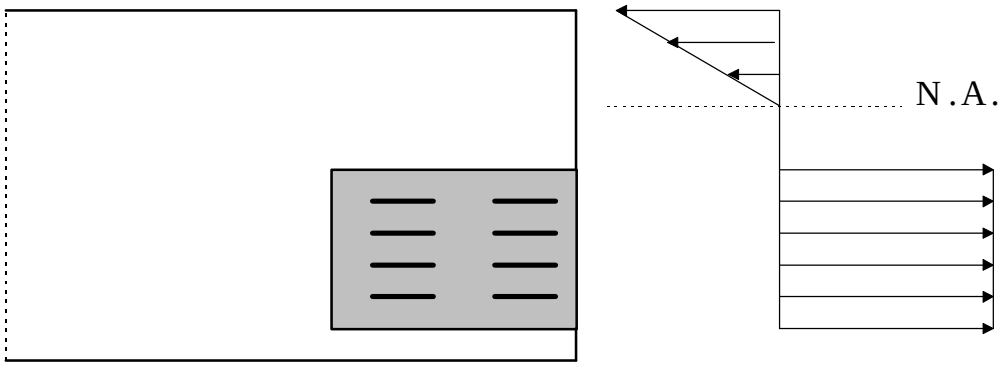

Figure 5.7 Plastic-elastic stress distribution for Noguchi s (1980) splice joint.

This model can be extended to splice joints with truss plates centered on the chord and subjected to tension and bending. This model, Model 2, uses the assumption that the wood has a linear stress distribution, similar to that in Model 1, but the steel is experiencing plastic behavior. For Model 2, all of the steel in tension is assumed to have reached maximum stress. For this model, the maximum stress in the steel will be assumed to equal the ultimate tensile stress of the steel. Figure 5.8 shows the assumed stress distribution for Model 2.

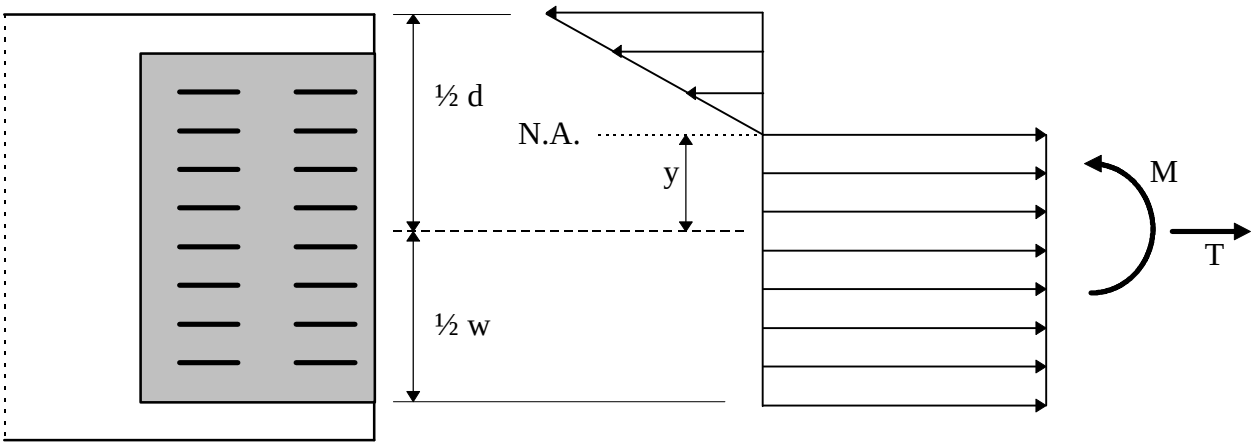

Figure 5.8 Assumed stress distribution for Model 2.

The assumptions for Model 2 are summarized below:

- The gap on the compression side of the joint closes and permits wood-to-wood contact.
- The compressive forces developed in the steel plates are negligible due to gap closure and consequent wood-to-wood bearing.
- The stress distribution for the wood in compression is linearly elastic, and the stress distribution for the steel in tension is plastic.
- The neutral axis lies within the truss plate.
- The maximum stress in the wood is equal to the ultimate compressive stress of the wood.
- The stress in the steel is equal to the ultimate tensile stress of the steel.
- The plane of the cross-section of the wood in compression remains plane when subjected to bending.

Although in this model the behavior of the steel is "plastic," this model does not follow the plastic theory of typical steel design procedures. Plastic design for steel materials usually assumes that the steel stress is equal to the yield stress of the steel, not the ultimate stress (Segui, 1994). However, in this model, the ultimate steel stress is used because the tested joints failed at the ultimate stress, and thus using the ultimate stress more accurately models the actual failure of the joints.

Figure 5.9 shows the equivalent forces for the stresses in the wood and steel. These forces, F_{wood} and F_{steel}, are shown in the opposite direction of the stresses because they represent the resistance of the joint to the applied loads T and M.

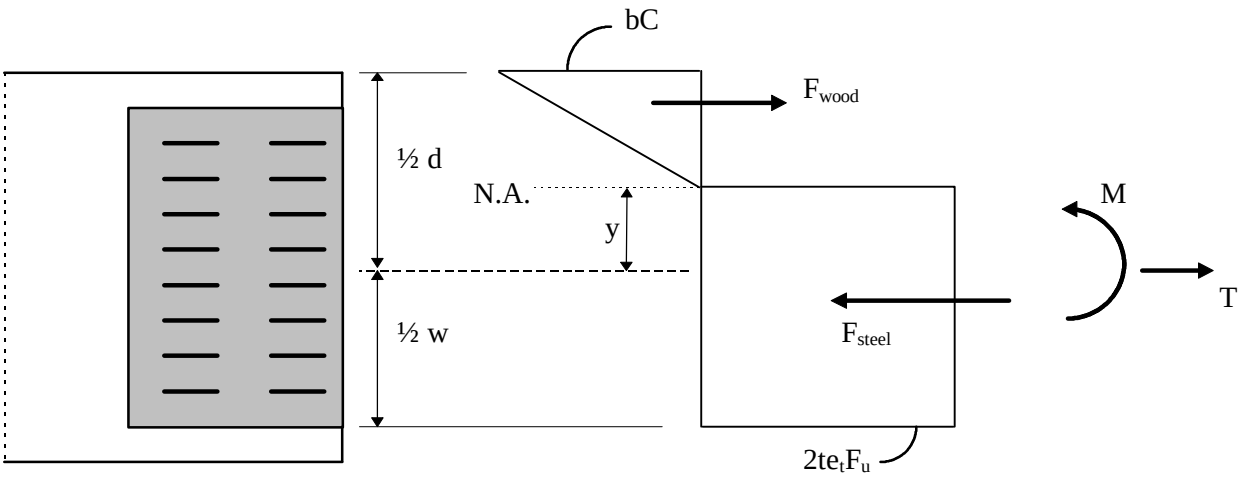

Figure 5.9 Stress distribution for Model 2. The forces F_{wood} and F_{steel} represent the resistance of the wood and the steel to the applied loads M and T.

Summing forces will give the location of the neutral axis. Equation 5.4 was derived for the location of the neutral axis:

$$(\Sigma F = 0) \qquad 2te_t F_u(\tfrac{1}{2}w + y) = \tfrac{1}{2}bC(\tfrac{1}{2}d - y) + T$$

$$y = \frac{\tfrac{1}{4}bdC + T - twe_t F_u}{2te_t F_u + \tfrac{1}{2}bC} \qquad (5.4)$$

Next, summing moments about the neutral axis yields Equation 5.5:

$$(\sum M = 0) \qquad M + Ty = \tfrac{1}{2} * 2te_t F_u (\tfrac{1}{2} w + y)^2 + \tfrac{1}{2} bC(\tfrac{1}{2} d - y)^2 * \tfrac{2}{3}$$

$$M + Ty = te_t F_u (\tfrac{1}{2} w + y)^2 + \tfrac{1}{3} bC(\tfrac{1}{2} d - y)^2 \qquad (5.5)$$

As in Model 1, these two equations can be solved simultaneously to find the ultimate moment that can be applied in addition to the specified tension force. Again, the compressive stress of the wood at the extreme edge must be defined. Assuming that the compressive stress of the wood at the extreme edge is equal to the median of the compressive strength for the grade of lumber used (4,139 psi), the test data collected were used to predict the moment. The actual applied tension force was used in the equations to solve for M, the predicted moment, and y, the location of the neutral axis. The ultimate stresses used for each of the three types of truss plates tested were the average ultimate stresses determined from the tension-only tests (Table 5.1). Table 5.3 shows that the predicted moment closely matches the actual moment for all test groups, with the maximum variation from the measured being 14%.

Table 5.3 Predicted ultimate moments using Model 2.

Test Group Description[a]	Number of Tests	T_{actual}[b] (lb.)	M_{actual}[b] (in.-lb.)	$M_{predicted}$ (in.-lb.)	$M_{predicted}/M_{actual}$	y (in.)
2x4, 20-G, 1.5	6	7,967	6,777	5,820	0.86	1.097
2x4, 20-G, 3.0	3	4,321	8,515	9,352	1.10	0.577
2x4, 20-G, 4.5	3	2,995	10,645	10,223	0.96	0.361
2x6, 20-G, 1.5	4	13,080	14,899	14,646	0.98	1.746
2x6, 20-G, 3.5	4	7,153	21,575	23,711	1.10	0.876
2x6, 16-G, 1.5	6	15,601	15,774	17,505	1.11	1.575
2x6, 16-G, 3.5	5	9,434	26,518	26,067	0.98	0.787

[a]Lumber size, plate gauge, and level of initial eccentricity (in.).
[b]The actual tension and moment values given are the averages for each test group.

5.3 Plastic-Plastic Stress Model (Model 3)

Model 3 is similar to the previous model, Model 2, except that the stress in the wood is also assumed to be plastic. This model is similar to Noguchi's fourth model, which was based on plastic behavior for both the steel and the wood. Of the five models discussed by Noguchi, he recommended that his fourth model be used to determine the moment capacity of splice joints with truss plates located below the neutral axis (Figure 5.1). The assumed stress distribution for Model 3 is shown in Figure 5.10. Again, the equivalent forces F_{wood} and F_{steel} are shown in the opposite direction of the stress blocks because they represent the resistance of the wood and the steel to the applied loads T and M.

The assumptions required for Model 3 are:

- The gap on the compression side of the joint closes and permits wood-to-wood contact.
- The compressive forces developed in the steel plates are negligible due to gap closure and consequent wood-to-wood bearing.
- The stress distribution for the wood in compression is plastic, and the stress distribution for the steel in tension is plastic.
- The neutral axis lies within the truss plate.
- The stress in the wood is equal to the ultimate compressive stress of the wood.
- The stress in the steel is equal to the ultimate tensile stress of the steel.

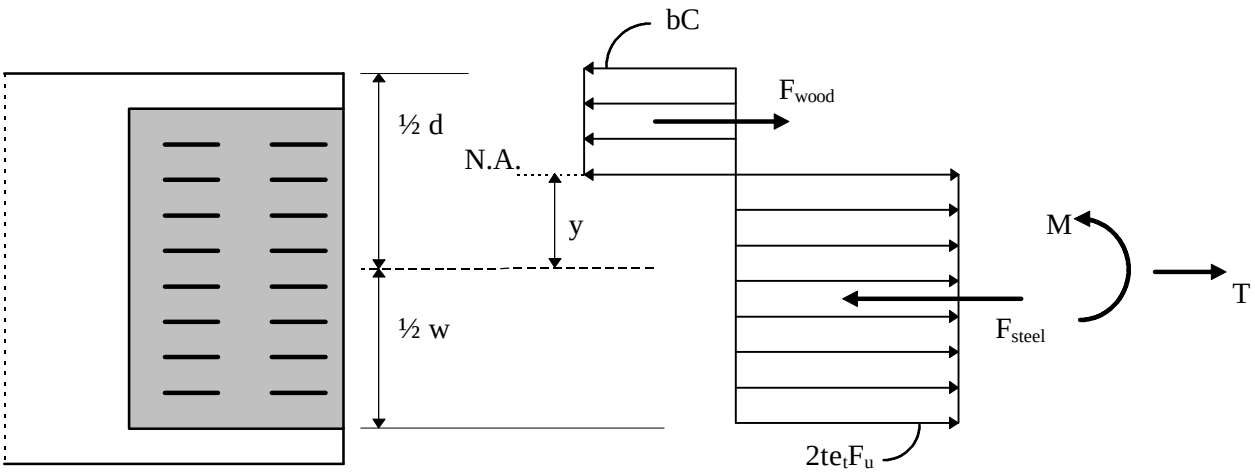

Figure 5.10 Stress distribution for Model 3. The forces F_{wood} and F_{steel} represent the resistance of the wood and the steel to the applied loads M and T.

The location of the neutral axis with respect to the centerline can be derived by summing forces, resulting in Equation 5.6:

$$(\sum F = 0) \qquad 2te_t F_u (½w + y) = bC(½d - y) + T$$

$$y = \frac{½bdC + T - twe_t F_u}{2te_t F_u + bC} \tag{5.6}$$

Summing moment about the neutral axis results in Equation 5.7:

$$(\sum M = 0) \qquad M + Ty = ½ * 2te_t F_u (½w + y)^2 + ½bC(½d - y)^2$$

$$M + Ty = te_t F_u (½w + y)^2 + ½bC(½d - y)^2 \tag{5.7}$$

These two equations can be solved simultaneously to find the maximum moment that can be applied in addition to the specified tension force. This model was used to predict the moment using the data collected from the tests. The compressive stress of the wood at the extreme edge was the median of the ultimate compressive strength for the grade of lumber used (4,139 psi). The applied ultimate tension force was used in the equations to solve for M, the predicted ultimate moment, and y, the location of the neutral axis. Table 5.4 shows the ratio of the predicted moment to the actual moment, and the location of the neutral axis, for each of the test groups. As seen in the table, all but one of the predicted values of M are greater than the actual moment load. A few of the test groups had predicted ultimate moment values that were more than 10% greater than the actual ultimate moment; however, this model seems to give good results.

Table 5.4 Predicted ultimate moments using Model 3.

Test Group Description[a]	Number of Tests	T_{actual}[b] (lb.)	M_{actual}[b] (in.-lb.)	$M_{predicted}$ (in.-lb.)	$M_{predicted}/M_{actual}$	y (in.)
2x4, 20-G, 1.5	6	7,967	6,777	6,052	0.89	1.303
2x4, 20-G, 3.0	3	4,321	8,515	10,128	1.19	0.933
2x4, 20-G, 4.5	3	2,995	10,645	11,276	1.06	0.798
2x6, 20-G, 1.5	4	13,080	14,899	15,199	1.02	2.060
2x6, 20-G, 3.5	4	7,153	21,575	25,639	1.19	1.463
2x6, 16-G, 1.5	6	15,601	15,774	18,325	1.16	1.909
2x6, 16-G, 3.5	5	9,434	26,518	28,356	1.07	1.345

[a]Lumber size, plate gauge, and level of initial eccentricity (in.).
[b]The actual tension and moment values given are the averages for each test group.

5.4 Comparison of Model 2 and Model 3

Of the three models proposed, Model 1 does not accurately fit the test data. Models 2 and 3 both fit the data very well, however. These results suggest that the steel is indeed behaving plastically. The difference between Models 2 and 3 is that Model 2 uses the assumption that the wood behaves elastically, while Model 3 uses the assumption that the wood behaves plastically. When the wood behaves plastically, it resists more load. This explains why the moments predicted using Model 3 are higher than those predicted by Model 2. As Table 5.5 shows, for each test group except the first, Model 2 gives predicted ultimate moments that are closer to the actual ultimate moments. The average ratio of predicted to ultimate moment for Model 2 is 1.01, with a coefficient of variation of 9%. The average ratio for Model 3 is 1.08, with a coefficient of variation of 10%. Thus, Model 2 is the more appropriate structural model for the design of splice joints subjected to tension and bending.

Table 5.5 Comparison of predicted ultimate moments for Model 2 and Model 3.

Test Group Description[a]	T_{actual}[b] (lb.)	M_{actual}[b] (in.-lb.)	Model 2 $M_{predicted}$ (in.-lb.)	Model 2 $M_{predicted}/M_{actual}$	Model 2 y (in.)	Model 3 $M_{predicted}$ (in.-lb.)	Model 3 $M_{predicted}/M_{actual}$	Model 3 y (in.)
2x4, 20-G, 1.5	7,967	6,777	5,820	0.86	1.097	6,052	0.89	1.303
2x4, 20-G, 3.0	4,321	8,515	9,352	1.10	0.577	10,128	1.19	0.933
2x4, 20-G, 4.5	2,995	10,645	10,223	0.96	0.361	11,276	1.06	0.798
2x6, 20-G, 1.5	13,080	14,899	14,646	0.98	1.746	15,199	1.02	2.060
2x6, 20-G, 3.5	7,153	21,575	23,711	1.10	0.876	25,639	1.19	1.463
2x6, 16-G, 1.5	15,601	15,774	17,505	1.11	1.575	18,325	1.16	1.909
2x6, 16-G, 3.5	9,434	26,518	26,067	0.98	0.787	28,356	1.07	1.345

[a]Lumber size, plate gauge, and level of initial eccentricity (in.).
[b]The actual tension and moment values given are the averages for each test group.

5.5 Other Models Discussed by Noguchi

Noguchi discussed five models, and three of them were adapted in this study as shown in Models 1, 2, and 3. The other two models discussed by Noguchi were not considered in this study. Noguchi's second model was based on elastic behavior for the steel and plastic behavior for the wood. This model was not adapted because it is not reasonable for the wood to reach plastic behavior before the steel. The fifth model investigated by Noguchi was originally proposed by Edlund (1971, as quoted by Noguchi, 1980). This model described the location of the neutral axis as existing at one-third of the depth of the chord when a splice joint is yielding due to moment. This model is empirical, and thus was not discussed here because a theoretical model was desired.

5.6 Model Evaluation Using Data from Other Studies

To verify the accuracy of both Model 2 and Model 3, data from two previous studies of moment in splice joints were used to predict the ultimate moment. Since Models 2 and 3 are very similar, the data will be used in both of them to verify that Model 2 is more accurate than Model 3.

5.6.1 Data from Wolfe s (1990) Study of Combined Tension and Bending

As discussed in the review of the literature, Wolfe (1990) tested the capacity of MPC wood truss splice joint connections for five combinations of bending and tension loading. Test specimens of 2x4 Southern Pine lumber and 3- by 5.25-in. 20-gauge truss plates were tested in tension only, bending only, and three levels of combined loading. Models 2 and 3 were used to predict the ultimate moment that can be applied in addition to the applied tension force for each of the combined loading test groups of Wolfe's study. Table 5.6 gives the results of the tests.

To use these data in the models, information about the truss plates and lumber used must be known. The grade of the lumber used was not given; a grade of No. 2 Southern Pine was assumed. The lumber was conditioned to a moisture content of 12%; therefore, the value of the ultimate compressive strength of the wood used in the models is 4,653 psi, found in Green and Evans (1987). The truss plates were 3 in. wide and 0.04 in. thick (20-gauge). The grade of steel used to manufacture the truss plates was not given. However, the grade can be determined from the tension-only tests. Wolfe determined a tension efficiency ratio, e_t, of 0.51. Using Equation 5.3 again, the ultimate stress of the steel can be determined:

$$F_u = \frac{T}{2twe_t}$$

Thus, for an average tension-only strength of 6,700 lbs, the ultimate tension stress, Fu, is 54.7 ksi. This is the value of the ultimate stress used in the models to predict the ultimate moment. Table 5.7 shows the predicted ultimate moments for each loading configuration, using both Models 2 and 3 to predict the moment.

Table 5.6 Wolfe (1990) results from testing splice joints in combined loading.

Applied Loading Level	Number of Tests	Tension Load[a] (lbs.)	Tension COV[b] (%)	Moment[a] (in.-lb.)	Moment COV[b] (%)
Tension only	20	6,700	6	----	----
Low moment, high tension	10	4,800	7	3,330	9
Medium moment and tension	10	2,530	5	6,040	3
High moment, low tension	12	940	5	7,110	5
Moment only	10	----	----	8,680	6

[a]The tension load and bending moment tabulated were measured at joint failure.
[b]Coefficient of variation.

Table 5.7 Predicted ultimate moments for Wolfe s joints using Models 2 and 3.

			Model 2			Model 3		
Initial Eccentricity	T_{actual} (lb.)	M_{actual} (in.-lb.)	$M_{predicted}$ (in.-lb.)	$M_{predicted}/M_{actual}$	y (in.)	$M_{predicted}$ (in.-lb.)	$M_{predicted}/M_{actual}$	y (in.)
0.875	4,800	3,330	2,974	0.89	1.320	3,067	0.92	1.483
2.625	2,530	6,040	5,811	0.96	0.924	6,154	1.02	1.237
9.875	940	7,110	7,371	1.04	0.646	7,983	1.12	1.064
moment only	-----	8,680	8,128	0.94	0.482	8,936	1.03	0.962

Both Models 2 and 3 predicted the ultimate moment for Wolfe's data very well. Model 3 appears to give a more accurate prediction of ultimate moments than Model 2 for all but the third test group (2.625 in. initial eccentricity). The average ratio of predicted to ultimate moment is 0.96 for Model 2, and the average ratio for Model 3 is 1.02. The coefficient of variation for Model 2 (6.5%) is lower than that for Model 3 (8.0%). It should be noted that the grade of lumber used was not given, and was assumed to be No. 2. If the actual grade used were higher than No. 2, then the predicted moments would be somewhat higher, and Model 2 would give closer predictions of the ultimate moment. Considering the coefficients of variation, Model 2 is more accurate than Model 3 in predicting the ultimate moments for Wolfe's data. Furthermore, the under-predicted ultimate moments of Model 2 are conservative, and thus provide a margin of safety.

5.6.2 Data from Soltis s (1985) Study of Partially Continuous Floor Joists

As described in the review of literature, Soltis (1985) tested several configurations of truss plate splice joints in bending-only as part of a study of partially continuous floor joists. A pair of truss plates were used to join two pieces of dimension lumber to form a partially continuous floor joist. The constructed joists were tested in bending using third-point loading. Although the purpose of his study was to investigate the feasibility of continuous floor joists, the data from the tests of the plate-connected joists can be used to determine how well Models 2 and 3 predict the ultimate moment for joints subjected to only moments. Even though the models developed in this study include a tension load, they may still accurately predict ultimate moments for splice joints subjected to bending moments without any tension loads.

The truss plates used were 16-gauge ASTM A446 Grade A steel. The efficiency ratio was not given, but the dimensions of the plate teeth and the plate tooth density were given. Considering the tooth density and dimensions, it was assumed that the plates used were Tee-Lok T-L-S plates, with an efficiency ratio of 0.75. This was determined by comparing the given tooth dimensions with ICBO Evaluation Service Inc. Evaluation Report No. 3777 (ICBO, 1992a), which describes the Tee-Lok truss plates.

Three species of wood were used in Soltis's study; Douglas Fir-Larch, Spruce-Pine-Fir, and White Woods. Most of the Douglas Fir-Larch specimens and the Spruce-Pine-Fir specimens failed in steel net-section. None of the White Woods specimens failed in steel net-section. Three sizes of Douglas Fir-Larch lumber were used; 2x6, 2x8, and 2x10. Two sizes of Spruce-Pine-Fir lumber were used; 2x6, and 2x8. The average moments at failure are shown in Table 5.8.

To use Soltis's data in the models, the ultimate compressive strength of the wood, C, used in the models must be estimated. The nominal design values for compression parallel-to-grain strength given in the National Design Specification (NDS) Supplement, Design Values for Wood Construction (AFPA, 1991), are based on the fifth percentile of the compression stress distribution. This means that 95% of the lumber for a given size and species will have a compression strength greater than the nominal design value, F_c, for that lumber size and species. Since Soltis's data represent ultimate moment values, a central value of the distribution of the ultimate compression strength, such as the median value, $\tilde{C}$, is desired. The median values for lumber strength are not readily available for any given species and grade; however, they can be estimated by using the compression parallel-to-grain strength data that is available.

Table 5.8 Soltis (1985) results from testing splice joints in bending.

Species Group	Joist Size	Truss Plate Size width-length (in.)	Number of Steel Net-section Failures	Average[a] Moment (in.-lb.)	COV[b] Moment (%)
Douglas Fir-Larch	2x6	5 x 20	5	34,980	4.2
	2x8	7 x 14	3	79,500	4.2
	2x10	9 x 18	2	121,860	3.4
Spruce-Pine-Fir	2x6	5 x 14	5	32,976	4.3
	2x8	7 x 12	2	70,380	23
White Woods	2x10	9 x 12	0	----	----

[a]The average ultimate moment includes only the specimens for each group that failed in steel net-section.
[b]Coefficient of variation

In addition to using the fifth percentile value to determine the nominal design value, F_c, several factors are applied to reduce the nominal value. For wood in compression parallel-to-grain, the fifth percentile value is reduced by a factor of 1.9 (ASTM D1990, 1996e). This factor includes a reduction for a safety factor and for the load duration effect. The nominal values are based on 2x12 lumber sizes, and must be multiplied by a size factor, C_F, to adjust for sizes other than 2x12. The median value of the compression parallel-to-grain strength, $\tilde{C}$, can be estimated as:

$$\tilde{C} = k * 1.9 C_F F_c \qquad (5.8)$$

where k is a constant that must be determined. Equation 5.8 can then be used to estimate the median of the ultimate compression parallel-to-grain strength from the nominal design value given in the NDS Supplement. The second term on the right-hand side of the equation, $1.9C_FF_c$, represents the fifth percentile value of the ultimate compression parallel-to-grain strength.

To determine an estimate of the constant, k, a published report of test data of various species and grades of full-size lumber was reviewed. Green and Evans (1987) summarized their test results of full-size visually graded dimension lumber. They gave summaries of the median and fifth percentile values of the compression parallel-to-grain strength for five species groups of commercial softwood lumber; Douglas Fir-Larch, Douglas Fir (South), Hem-Fir, Mixed Southern Pine, and Southern Pine. Table 5.9 shows the combinations of moisture content, lumber size, and lumber grade tested for each of the five species groups. The sample sizes of each combination of size, grade, and moisture content varied among the five species groups. For most of the groups, sample sizes ranged from about 250 to 410. For Douglas Fir (South), the sample sizes were about 40 to 80. For Mixed Southern Pine, the sample sizes were about 150. The Green and Evans (1987) database gives the most recent and comprehensive information available on the properties of full-size lumber used in the United States.

Since $1.9C_FF_c$ represents the fifth percentile, Equation 5.8 can be re-written as Equation 5.9:

$$k = \frac{\tilde{C}}{C_{0.05}} \qquad (5.9)$$

where:

$\tilde{C}$ is the median value of the ultimate compression parallel-to-grain strength,
$C_{0.05}$ is the fifth percentile value of the ultimate compression strength, and
k is the ratio of the median to the fifth percentile.

This ratio, k, was calculated for each lumber size and grade combination for both the 12% and 15% moisture contents for the five species groups reported by Green and Evans. Appendix B gives a table showing the median, the fifth percentile, and the ratio, k, for each of the combinations.

Table 5.9 Combinations of moisture content, lumber size, and lumber grade tested in compression parallel-to-grain and reported by Green and Evans (1987).

Moisture Content (%)	Lumber Size[a]		
	2x4	2x8	2x10
12	Select Structural No. 1 & Better No. 2	Select Structural No. 1 & Better No. 2	Select Structural No. 1 & Better No. 2
15	Select Structural No. 1 & Better No. 2	Select Structural No. 1 & Better No. 2	Select Structural No. 1 & Better No. 2
23	Select Structural No. 1 & Better No. 2	Select Structural No. 1 & Better No. 2	Select Structural No. 1 & Better No. 2

[a]For the Mixed Southern Pine species group, the lumber sizes tested were 2x4, 2x6, and 2x8.

The ratio, k, for combinations of the 23% moisture content groups was not calculated because only KD19 lumber was considered. The lumber used in wood truss fabrication is usually KD19 lumber, and the average moisture content at the time of the lumber manufacturing is expected to be 15%. Framing lumber is expected to dry in service to an average moisture content of about 12%. Thus, the 12 and 15% moisture content groups were considered for estimating the ratio of $\tilde{C}$ to $C_{0.05}$.

The average ratio, k, for each of the five species groups is given in the tables in Appendix B. The average ratios for the five species groups ranged from 1.32 to 1.41. The five average ratios were then averaged together. The overall average ratio of the median to the fifth percentile was 1.36. This value of k is recommended for use in Equation 5.8 when determining the median value of the ultimate compression parallel-to-grain strength of dimension lumber. Equation 5.8 is re-written below as Equation 5.10:

$$\tilde{C} = 1.36(1.9 C_F F_c) \qquad (5.10)$$

Thus, for Soltis's data, Equation 5.10 was used to estimate the median of the ultimate compression parallel-to-grain strength, $\tilde{C}$, for each of the three sizes of the Douglas Fir-Larch test joints and the two sizes of Spruce-Pine-Fir test joints, using the appropriate values of the nominal strength, F_c, and the size factor, C_F, from the NDS Supplement. The estimated values are shown in Table 5.10

The truss plates used in Soltis's study were fabricated from ASTM A446 Grade A steel. While the nominal ultimate tensile strength, F_u, of Grade A steel is 45 ksi, it has been shown that steel used in the manufacture of truss plates usually exceeds the nominal strengths by considerable amounts (Skaggs et al., 1995). From Skaggs et al., the average ultimate strength for Grade A steel used by one truss plate manufacturer was 53.94 ksi, representing a ratio of average ultimate tensile strength, $\overline{F}_u$, to nominal ultimate tensile strength, F_u, of 1.2. Kennedy and Gad Aly (1980) reported a range of 1.03 to 1.22 for this ratio for structural steels. For predicting the ultimate moments for Soltis's data, the ratio of $\overline{F}_u$ to F_u was assumed to be 1.2, and thus a value of 54 ksi (equal to 1.2 times 45 ksi) was assumed for the average ultimate tensile strength, $\overline{F}_u$, of the truss plates.

The equations for Models 2 and 3 were used to estimate the ultimate moments for the 2x6, 2x8, and 2x10 Douglas Fir-Larch joint configurations, and for the 2x6 and 2x8 Spruce-Pine-Fir joint configurations. The predicted ultimate moments for each joint configuration are shown in Table 5.10.

Table 5.10 Predicted ultimate moments for Soltis s (1985) test splice joints using Models 2 and 3.

			Model 2			Model 3		
Species and Size	Actual Moment[c] (in.-lb.)	Wood Strength, $\tilde{C}$ (psi)	Predicted Moment (in.-lb.)	$M_{predicted}/M_{actual}$	y (in.)	Predicted Moment (in.-lb.)	$M_{predicted}/M_{actual}$	y (in.)
D. F-L[a] 2x6	34,980	3,695	29,058	0.83	-0.552	35,042	1.00	0.342
D. F-L 2x8	79,500	3,527	52,119	0.66	-0.933	63,162	0.79	0.274
D. F-L 2x10	121,860	3,359	83,090	0.68	-1.315	101,218	0.83	0.222
S-P-F[b] 2x6	32,976	3,127	26,350	0.80	-0.752	32,344	0.98	0.123
S-P-F 2x8	70,380	2,985	47,170	0.67	-1.201	58,187	0.83	-0.023

[a]Douglas Fir-Larch.
[b]Spruce-Pine-Fir.
[c]The actual moment listed is the average actual moment of the test joints that had steel net-section failures, for each combination of species and lumber size.

Both Models 2 and 3 did not predict the ultimate moments for Soltis's data as well as they did for the data from this study. The average ratio of predicted to ultimate moment for Model 2 was 0.73, with a coefficient of variation of 11%. The average ratio for Model 3 was 0.89, with a coefficient of variation of 11%. It may appear that Model 3 more accurately predicts the ultimate moment; however, the assumption that the type of truss plates used were Tee-Lok T-L-S, with an efficiency ratio of 75%, may not be correct. Furthermore, the objective of this study was to accurately model typical bottom chord splice joints. Typical splice joints will always experience a tension load, and usually significant moment as well. It should be emphasized that the three models presented in this study were developed for splice joints subjected to tension and bending. Thus, considering the accurate moment predictions for both the data from this study and Wolfe's data, Model 2 is the most appropriate model for bottom chord splice joints.

5.7 Development of a Design Method Based on Model 2

The equations given for Model 2, Equations 5.4 and 5.5, are for ultimate capacity values, not design values. They must be modified before they can be used for designing the steel net-section of splice joints. One possible way to use the equations for design purposes is to use the moment at the joint, M, which is determined from the engineering analysis of the truss, to calculate the ultimate tension load, T_{ult}, that may be applied in addition to the moment M. This ultimate load, T_{ult}, is the tension load that will cause steel net-section failure of the joint when applied in conjunction with the moment M. A safety factor can then be applied to the ultimate tension, T_{ult}, to get an allowable tension load, $T_{all,M}$. (The subscript, "M", signifies that this allowable tension load is applied in conjunction with a moment. This subscript is to differentiate $T_{all,M}$ from $T_{all,T}$, which is the allowable tension capacity for truss plate joints subjected to only a tension load.) The applied tension load, T, which is determined from the engineering analysis of the truss, can be compared to $T_{all,M}$ to ensure that the applied tension load does not exceed the allowable tension load.

A safety factor can also be applied to the applied moment, M, by first using the equations to calculate the ultimate moment capacity of the joint, M_{ult}, by setting T in the equations equal to zero. Then the ultimate moment can be reduced by a safety factor to get M_{all}, the allowable moment, which can be compared to M, the applied moment, to ensure that the applied moment does not exceed the allowable moment.

The median of the ultimate compressive strength of the wood for loading parallel-to-grain, $\tilde{C}$, can be estimated using Equation 5.11, which was discussed earlier in Section 5.6.2 as Equation 5.10:

$$\tilde{C} = 1.36(1.9 C_F F_c) \qquad (5.11)$$

The size factor, C_F, and the nominal design value for compression parallel-to-grain, F_c, for the size and grade of lumber used for the joint being designed, can be found in the NDS Supplement. As discussed in Section 5.6.2, a value of 1.36 for k, the ratio of the median to the fifth percentile of the compression parallel-to-grain strength for dimension lumber, is recommended for design purposes.

Equations 5.4 and 5.5 have been re-written as Equations 5.12 and 5.13:

$$y = \frac{\frac{1}{4} bd\tilde{C} + T_{ult} - twe_t F_u}{2te_t F_u + \frac{1}{2} b\tilde{C}} \tag{5.12}$$

$$M + T_{ult} y = te_t F_u (\tfrac{1}{2} w + y)^2 + \tfrac{1}{3} b\tilde{C} (\tfrac{1}{2} d - y)^2 \tag{5.13}$$

These two equations can be solved simultaneously, using the moment M from the truss analysis and $\tilde{C}$ from Equation 5.11, to determine the ultimate tension load, T_{ult}, that will cause failure when applied with the moment M. The calculated location of the neutral axis, y, should be checked to ensure that it lies within the truss plate since this is a required assumption for Model 2. If it does not lie within the truss plate for a splice joint, the equations derived for Model 2 are invalid and cannot be used for that splice joint. To ensure that the neutral axis lies within the truss plate, Equation 5.14 can be used:

$$|y| \le \tfrac{1}{2} w \tag{5.14}$$

where w is the width of the truss plate.

The absolute value of y is used because it is possible for the neutral axis to lie below the centerline of the chord member. Such a case would not invalidate the equations of Model 2 as long as the neutral axis is still located within the truss plate.

Next, a safety factor must be applied to the ultimate tension load to determine the allowable tension load, $T_{all,M}$. For allowable stress design (ASD) of steel structures, the safety factor used for the ultimate tensile strength of steel is 2.0 (Segui, 1994). That is, the applied tensile stress must be not exceed one-half of the ultimate tensile strength, F_u. Thus, the allowable tension load, $T_{all,M}$, is equal to one-half of the ultimate tension load, T_{ult}. Equation 5.15 shows this relationship:

$$T_{all,M} = 0.5\, T_{ult} \tag{5.15}$$

This is the maximum tension load that may be safely applied when the applied moment, M, is present. In addition, the applied tension load, T, should also be checked against the allowable tension-only capacity of the steel net-section of the truss plates, $T_{all,T}$, to prevent the possibility of

a calculating a value of $T_{all,M}$ that is greater than $T_{all,T}$. This capacity can be determined using Equation 5.16:

$$T_{all,T} = 2tw(0.6F_y)e_t \tag{5.16}$$

Thus, the allowable tension load for splice joints subjected to tension and bending, T_{all}, is the lessor of $T_{all,M}$ and $T_{all,T}$, as shown in Equation 5.17:

$$T_{all} = \min\begin{cases} T_{all,M} \\ T_{all,T} \end{cases} \tag{5.17}$$

For high-strength grades of steel, such as ASTM A653 Gr. 60 steel, $T_{all,M}$ will generally control the design. For mild grades of steel and relatively low moments, $T_{all,T}$ will control the design. The ratio of the ultimate tensile strength, F_u, to the yield strength, F_y, is higher for mild steel grades than for high-strength steel grades, and this ratio affects the relative sizes of $T_{all,M}$ and $T_{all,T}$. Since the equation for $T_{all,M}$ is based on the ultimate tensile strength, F_u, a value of $T_{all,M}$ that is greater than the value of $T_{all,T}$ will result for steels with high F_u to F_y ratios. Generally, for most high-strength grades of steel, $T_{all,M}$ will be the lessor value. Later in this chapter, several graphs are shown that better illustrate this concept.

Finally, the applied moment, M, can be checked against M_{all}, the allowable moment, to provide a factor of safety for the case of a large applied moment and a low applied tension. A case of this type may occur when a concentrated load is applied to the bottom chord of a truss. The ultimate moment, M_{ult}, can be determined by setting T_{ult} equal to zero in Equations 5.12 and 5.13. These equations are re-written below as Equations 5.18 and 5.19:

$$y^* = \frac{¼\,bd\tilde{C} - twe_tF_u}{2te_tF_u + ½\,b\tilde{C}} \tag{5.18}$$

$$M_{ult} = te_tF_u(½\,w + y^*)^2 + ⅓\,b\tilde{C}(½\,d - y^*)^2 \tag{5.19}$$

where M_{ult} is the ultimate moment, and y^* is the location of the neutral axis with respect to the chord centerline when the joint is subjected to only M_{ult}. This value of the location of the neutral axis will not be the same as the value calculated from Equation 5.12, and it is only used for the calculation of M_{ult}. This value of the neutral axis should also be checked to ensure that it lies within the truss plate; Equation 5.14 can also be used for this check.

The same safety factor of 2.0 that applies to the tension also applies to the moment. The allowable moment, M_{all}, is determined using Equation 5.20:

$$M_{all} = 0.5\, M_{ult} \qquad (5.20)$$

These equations, Equations 5.11 through 5.20, can be used to determine the allowable tension load, T_{all}, that may be applied to a splice joint in addition to the applied moment, M. An example will illustrate the use of these equations.

5.7.1 Example of a Splice Joint Design Using the Proposed Design Procedure

A 2x4 pitched roof truss design is being checked. From the truss engineering analysis, the applied moment, M, at the bottom chord splice joint is 4,500 in.-lb., and the applied tension, T, is 4,000 lb. The lumber used for the bottom chord is No. 2 KD19 Southern Pine. The truss plates used for the splice joint are 3.28x8.75 20-gauge ASTM A653 Grade 60 steel, with an efficiency ratio of 0.71. Is the steel net-section of these plates adequate for the applied tension and bending loads?

Solution:

The required design checks are summarized:

- The location of the neutral axis, y, must lie within the truss plate:

  $$|y| \le \tfrac{1}{2}\, w$$

- The applied tension load, T, must be not exceed the allowable tension load, T_{all}:

  $$T \le T_{all}$$

  $$\text{where: } T_{all} = \min\begin{cases} T_{all,M} \\ T_{all,T} \end{cases}$$

- The applied moment, M, must not exceed the allowable moment, M_{all}:

  $$M \le M_{all}$$

First, the median value of the ultimate compressive strength, $\tilde{C}$, is estimated using Equation 5.11. From the NDS Supplement, for 2x4 No. 2 KD19 Southern Pine lumber, the nominal design value for compression parallel-to-grain, F_c, is 1,650 psi, and the size factor, C_F, is 1.0. As mentioned

earlier, for design purposes k, the ratio of the median to the fifth percentile, is assumed to be 1.36 for all grades and species groups of dimension lumber.

$$\tilde{C} = 1.36(1.9C_F F_c) = 1.36(1.9*1.0*1,650) = 4,264 \text{ psi}$$

Next, Equations 5.12 and 5.13 are solved simultaneously to find y and T_{ult}:

$$y = \frac{\frac{1}{4} bd\tilde{C} + T_{ult} - twe_t F_u}{2te_t F_u + \frac{1}{2} b\tilde{C}} = \frac{\frac{1}{4}*1.5*3.5*4,264 + T_{ult} - 0.036*3.28*0.71*70,000}{2*0.036*0.71*70,000 + \frac{1}{2}*1.5*4,264}$$

$$M + T_{ult} y = te_t F_u (\tfrac{1}{2} w + y)^2 + \tfrac{1}{3} b\tilde{C}(\tfrac{1}{2} d - y)^2$$

$$4,500 + T_{ult} * y = 0.036*0.71*70,000(\tfrac{1}{2}*3.28 + y)^2 + \tfrac{1}{3}*1.5*4,264(\tfrac{1}{2}*3.5 - y)^2$$

y = 1.255 in.

T_{ult} = 8,799 lb.

Equation 5.14 is used to ensure that the location of the neutral axis, y, lies within the truss plate:

$$|y| \le \tfrac{1}{2} w$$

$$1.255 \le \tfrac{1}{2} 3.28 = 1.64 \qquad \textbf{OK}$$

Next, Equation 5.15 is used to convert T_{ult} into $T_{all,M}$:

$$T_{all,M} = 0.5\, T_{ult} = 0.5*8,779$$

$T_{all,M}$ = 4,390 lb.

Equation 5.16 is used to determine $T_{all,T}$, the allowable tension-only capacity of the truss plates:

$$T_{all,T} = 2tw(0.6F_y)e_t = 2*0.036*3.28*(0.6*60,000)*0.71$$

$T_{all,T}$ = 6,036 lb.

Thus, the allowable tension load for splice joints subjected to tension and bending, T_{all}, is the lessor of $T_{all,M}$ and $T_{all,T}$:

$$T_{all} = \min\begin{cases} T_{all,M} = 4{,}390 \\ T_{all,T} = 6{,}036 \end{cases}$$

T_{all} = 4,390 lb.

The applied tension load is checked to ensure that it is less than the allowable:

T = 4,000 lb. < T_{all} = 4,390 lb. **OK**

Next, the ultimate moment, M_{ult}, is calculated using Equations 5.18 and 5.19:

$$y^* = \frac{\frac{1}{4} bd\tilde{C} - twe_t F_u}{2te_t F_u + \frac{1}{2} b\tilde{C}} = \frac{\frac{1}{4} * 1.5 * 3.5 * 4{,}264 - 0.036 * 3.28 * 0.71 * 70{,}000}{2 * 0.036 * 0.71 * 70{,}000 + \frac{1}{2} * 1.5 * 4{,}264}$$

y^* = -0.0402 in.

$$M_{ult} = te_t F_u (\tfrac{1}{2} w + y^*)^2 + \tfrac{1}{3} b\tilde{C} (\tfrac{1}{2} d - y^*)^2$$

$$M_{ult} = 0.036 * 0.71 * 70{,}000 * (\tfrac{1}{2} * 3.28 - 0.0402)^2 + \tfrac{1}{3} * 1.5 * 4{,}264 * (\tfrac{1}{2} * 3.5 + 0.0402)^2$$

M_{ult} = 11,412 in.-lb.

Equation 5.14 is again used to ensure that the location of the neutral axis, y^*, lies within the truss plate:

$$|y^*| \le \tfrac{1}{2} w$$

$$-0.0402 \le \tfrac{1}{2} 3.28 = 1.64 \quad \textbf{OK}$$

The allowable moment, M_{all}, is calculated using Equation 5.20:

$$M_{all} = 0.5 M_{ult} = 0.5 * 11{,}412$$

M_{all} = 5,706 in.-lb.

The applied moment is checked to ensure that it is less than the allowable:

M = 4,500 in.-lb. < M_{all} = 5,706 in.-lb. **OK**

Thus, the design checks. The steel net-section of the truss plates selected for the splice joint is adequate for the applied moment and tension loads.

It should be noted that the calculated value of 4,390 lb. for the allowable tension load, T_{all}, is applicable only when the applied moment, M, equals 4,500 in.-lb. Thus, a different applied moment will result in a different allowable tension load. The calculated allowable moment, M_{all}, represents the maximum moment capacity of the splice joint; this value, 5,706 in.-lb., is the largest moment that may be safely applied when any tension load is applied.

5.7.2 Design Example Using Other Design Methods

The same truss joint analyzed in the above example was also analyzed using two alternative design methods that may be used for designing splice joints subjected to combined bending and tension. These design methods were presented earlier in the review of literature (Chapter 2). Each method uses an equation to convert the applied moment, M, into an "equivalent" tension load, T^*, which is then added to the applied tension load, T. The resulting total tension load is then used to determine the required plate size.

The first design method is given in the ANSI/TPI 1-1995 Commentary (TPI, 1995b), and was shown earlier as Equation 2.1:

$$T^* = \frac{3M}{2d}$$

where:

T^* is the tension force that is equivalent to the applied moment,
M is the applied moment, and
d is the depth of the truss chord.

Using the depth of the truss chord in the above equation is not a consistent measure of the joint performance for comparison of the models. It is more logical (and more conservative) to use w, the width of the truss plates, in place of d, the depth of the truss chord. Thus, the design method of the ANSI/TPI 1-1995 Commentary will be rewritten as Equation 5.21, and this equation will be used in this thesis:

$$T^* = \frac{3M}{2w} \qquad (5.21)$$

This equivalent tension load is then subtracted from the allowable tension-only load, $T_{all,T}$, to determine the allowable tension load, $T_{all,Com}$, that may be safely applied in addition to the applied moment, M. The subscript "Com" denotes that this allowable tension load was calculated using the ANSI/TPI 1-1995 ***Com***mentary method. Equation 5.22 gives $T_{all,Com}$:

$$T_{all,Com} = T_{all,T} - T^{*} \qquad (5.22)$$

The second design method was shown earlier as Equation 2.2:

$$T^{*} = \frac{6M}{d}$$

where d is the depth of the truss chord. Again, the use of the chord depth, d, is illogical, and thus the plate width, w, will be used for this design method. Therefore, this design method is re-written as Equation 5.23.

$$T^{*} = \frac{6M}{w} \qquad (5.23)$$

As with the ANSI/TPI Commentary design method, this equivalent tension load is subtracted from the allowable tension-only load, $T_{all,T}$, to determine the allowable tension load, $T_{all,6}$, that may be safely applied in addition to the applied moment, M. The subscript "6" denotes that this allowable tension load was calculated using the ***6***M/w method. Equation 5.24 gives $T_{all,6}$:

$$T_{all,6} = T_{all,T} - T^{*} \qquad (5.24)$$

Later in this thesis, this design method will be shown to be overly conservative and unsuitable for design.

To check the splice joint design given in the above example using these two design methods, the allowable design value for tension-only loading, $T_{all,T}$ is required. This value, 6,036 lb., was found earlier using Equation 5.16

.

The design method of the ANSI/TPI Commentary (Equation 5.21) will be considered first. The applied moment, M, is converted into the "equivalent" tension load, T^{*}:

$$T^{*} = \frac{3M}{2w} = \frac{3*4{,}500}{2*3.28}$$

$\mathbf{T^* = 2{,}058\ lb.}$

Next, this tension load is subtracted from the allowable tension-only load, $T_{all,T}$, to determine the maximum allowable tension load, $T_{all,Com}$, that may be safely applied in addition to the applied moment, M:

$T_{all,Com} = T_{all,T} - T^* = 6{,}036 - 2{,}058$

$\mathbf{T_{all,Com} = 3{,}978\ lb.}$

Finally, the applied tension load, T, is checked to ensure that it does not exceed $T_{all,Com}$, the allowable tension load that may be applied in addition to the 4,500 in.-lb. moment:

$T = 4{,}000\ lb. > T_{all,Com} = 3{,}978\ lb.$ **NG**

Thus, the splice joint design is not adequate. This method gives an allowable tension load (3,978 lb.) that is relatively close to that calculated (4,390 lb.) using the proposed design method of this study; in fact, the allowable tension load of this method is only 10% less than that from the proposed method.

Next, the same steps will be repeated using the second of the two alternative design methods. Equation 5.23 is used to determine the "equivalent" tension load, T^*, caused by the moment, M:

$$T^* = \frac{6M}{w} = \frac{6*4{,}500}{3.28}$$

$\mathbf{T^* = 8{,}232\ lb.}$

Note that this "equivalent" tension load (8,232 lb.) is four times that calculated using Equation 5.20 of the ANSI/TPI Commentary method (2,058 lb.). The allowable tension load, T_{all}, that may be safely applied in addition to the 4,500 in.-lb. moment is calculated from Equation 5.24:

$T_{all,6} = T_{all,T} - T^* = 6{,}036 - 8{,}232$

$\mathbf{T_{all,6} = -2{,}196\ lb.}$

The calculated allowable tension load is negative, indicating that for this method, a moment of 4,500 in.-lb. overstresses the joint, and no tension load may be safely added in addition to the moment. This method is overly conservative, and is not recommended for design purposes.

5.8 Comparison of Proposed Design Procedure to Other Design Methods

To illustrate how the three design methods differ, several graphs were created. Each graph shows how the allowable tension load decreases as the applied moment increases from zero to the maximum allowable moment, M_{all}, for each of the three design methods. Table 5.11 describes the truss plates and lumber used for the splice joints for each of three figures.

Table 5.11 Properties and dimensions of the splice joints used to create Figures 5.11, 5.12, and 5.13.

Truss Plates	Steel Grade	Gauge (in.)	Plate Width (in.)	Plate Length (in.)	Lumber Size	Lumber Species Group	Lumber Grade
Alpine HS2510	60[a]	20 (0.036)	3.28	8.75	2x4	S. Pine	No. 2
MiTek PTH	33[b]	16 (0.058)	7.0	10	2x8	S. Pine	No. 2
Tee-Lok T-L-S	37[c]	16 (0.058)	5.0	10.25	2x6	D. F-L	No. 1

[a]ASTM A653 HSLA Grade 60 steel
[b]ASTM A653 SQ Grade 33 steel
[c]ASTM A653 SQ Grade 37 steel

Figure 5.11 was created for the same Alpine 20-gauge truss plates and 2x4 lumber that was used for the 2x4 splice joints tested in this study. The maximum applied moment shown on the x-axis of the graph, 5,700 in.-lb., is the allowable moment-only capacity, M_{all}, calculated from Equation 5.20 of the proposed design method. The curve marked "6M/w" represents the allowable tension load, $T_{all,6}$, calculated using the 6M/w design method. As demonstrated by the curve, this method is overly conservative, and should not be used for design. The curve marked "3M/2w" is the allowable tension load, $T_{all,Com}$, calculated using the design method of the ANSI/TPI Commentary. This design is generally slightly conservative in comparison to the proposed design method for this splice joint configuration.

Figure 5.12 shows the same curves for a different splice joint configuration. These curves were developed for MiTek PTH 16-gauge truss plates, made from ATSM A653 Grade 33 steel. The tension efficiency ratio, e_t, for theses plates is 0.62. These plates were described in ICBO Evaluation Service Inc. Evaluation Report No. 1591 (ICBO, 1992b). The first part of the curve

for the proposed design method is a horizontal line, representing an allowable tension load equal to 9,968 lb. The horizontal part of the curve indicates that the allowable tension load from the proposed method is controlled by the allowable tension-only capacity, $T_{all,T}$, of the truss plates. As explained earlier, $T_{all,T}$ controls because these truss plates are made from mild steel and therefore have a high ratio of ultimate steel strength to yield strength (F_u to F_y). Thus, for mild steel plates and relatively low moments, the allowable tension load, $T_{all,M}$, calculated from Equation 5.15 of the proposed design method, will be higher than the allowable tension-only capacity, $T_{all,T}$, and thus $T_{all,T}$ will control the design.

For Figure 5.13, 16-gauge Tee-Lok plates and 2x6 No. 1 KD19 Douglas Fir-Larch lumber were used for the splice joint. These plates were described in ICBO Evaluation Service Inc. Evaluation Report No. 3777 (ICBO, 1992a). The steel grade was ASTM A653 SQ Grade 37 steel, which is a mild steel, and thus the first part of the curve for the proposed design method is controlled by the tension-only capacity, $T_{all,T}$. As shown by the horizontal part of the curve, this splice joint configuration has a tension-only capacity of about 10,000 lb. Any moment up to about 10,000 in.-lb. can be safely added in addition to the 10,000 lb. tension load. The ratio of F_u to F_y for these Grade 37 steel plates is 1.46, which is relatively high. Thus, $T_{all,T}$ controls the design for applied moments up to 10,000 in.-lb.

Figures 5.12 and 5.13 demonstrate that the design method of the ANSI/TPI Commentary (3M/2w) is conservative for truss plates made from mild steels. Also, these graphs show that the 6M/d design method is too conservative, and is not an appropriate model for determining the steel net-section capacity of bottom chord splice joints.

Although the proposed design procedure is recommended for determining the steel net-section capacity of splice joints subjected to combined tension and bending, the simpler method of the ANSI/TPI Commentary gives slightly conservative estimates of the steel net-section capacity, as illustrated by the three graphs. The ANSI/TPI Commentary design method may be preferred over the proposed design procedure in cases where a conservative estimate of the steel net-section capacity is acceptable.

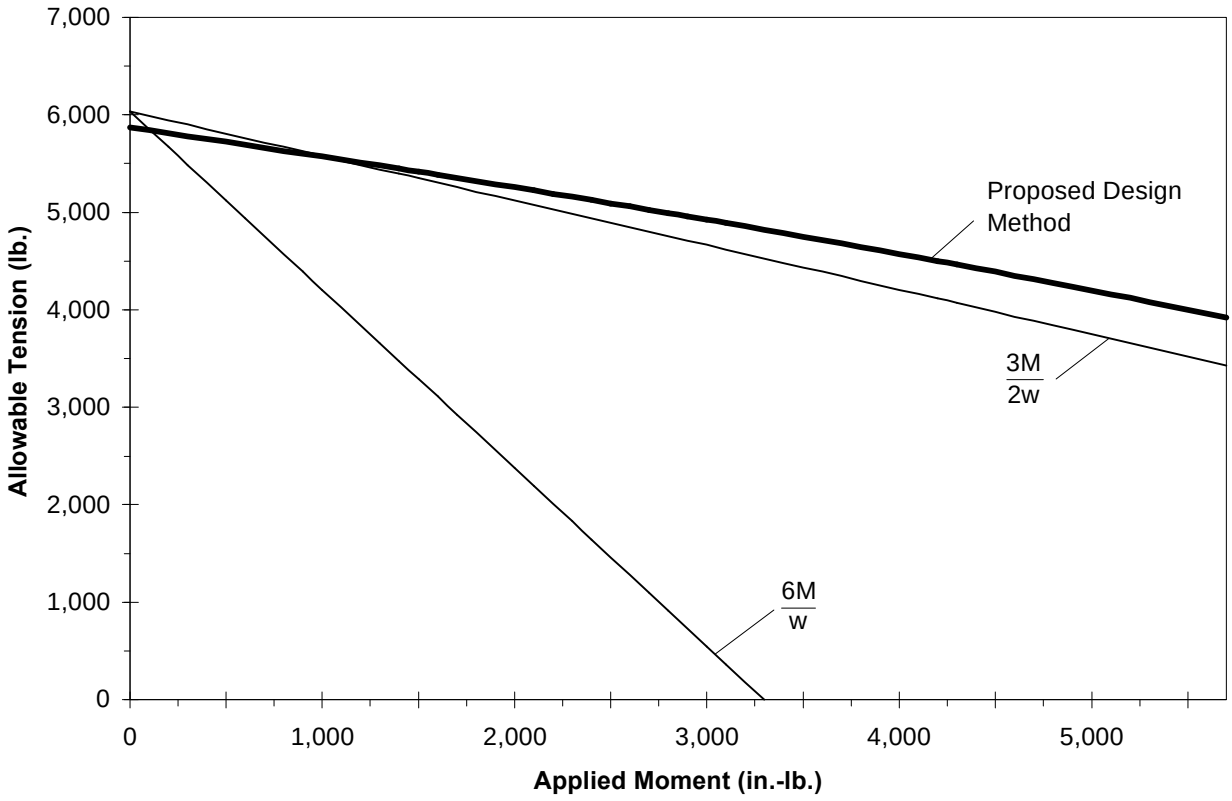

Figure 5.11 Comparison of the three design methods using Alpine HS2510 Grade 60 20-gauge truss plates and 2x4 No. 2 KD19 Southern Pine lumber.

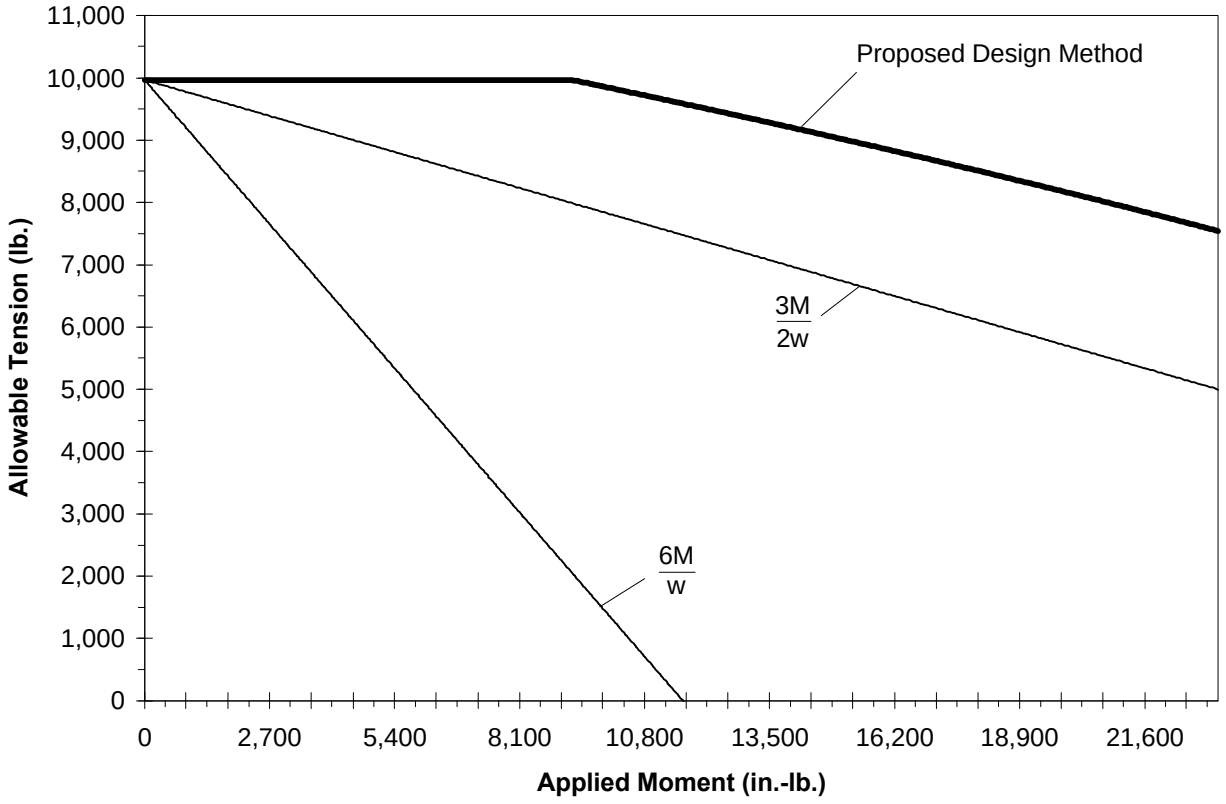

Figure 5.12 Comparison of the three design methods using MiTek PTH Grade 33 16-gauge truss plates and 2x8 No. 2 KD19 Southern Pine lumber.

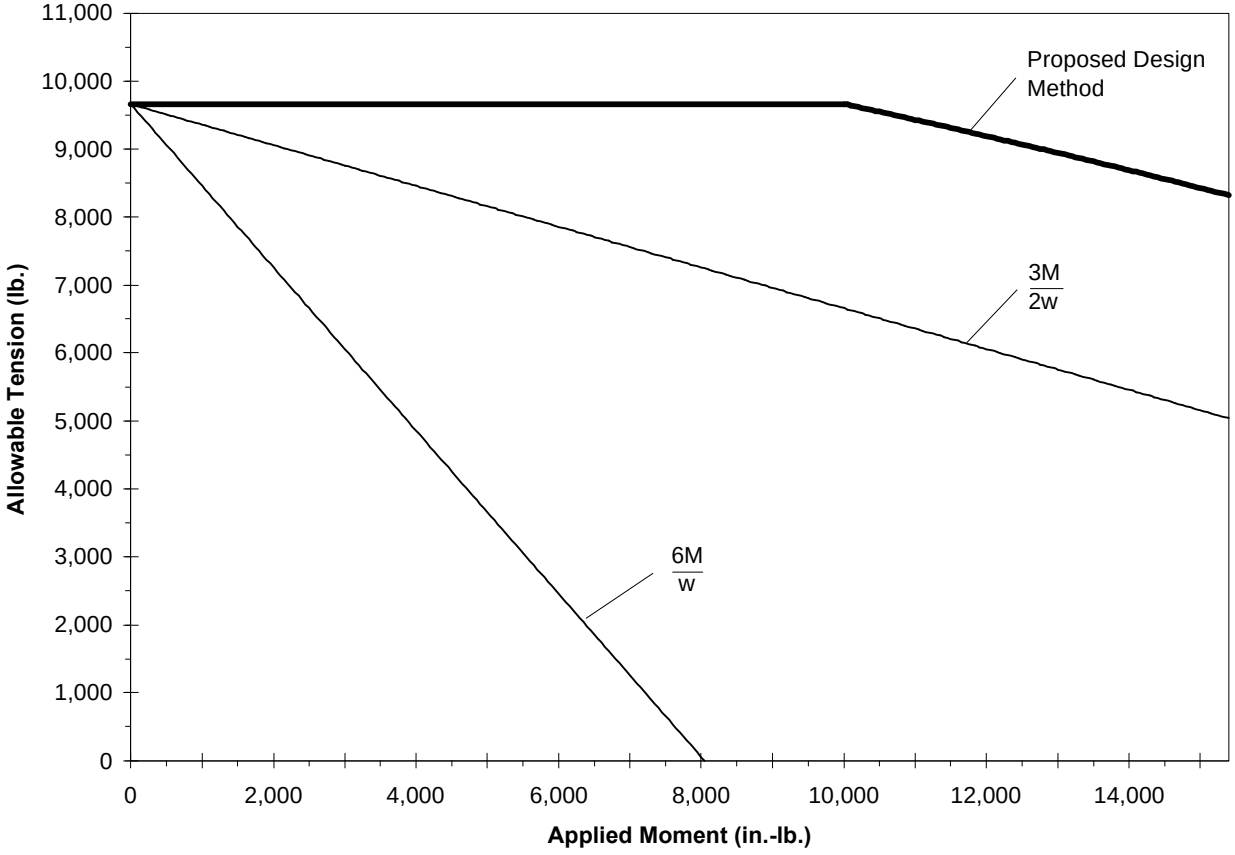

Figure 5.13 Comparison of the three design methods for Tee-Lok T-L-S Grade 37 16-gauge truss plates with 2x6 No. 1 KD19 Douglas Fir-Larch lumber.

5.8 Recommendations for a Standard Test Method for Combined Tension and Bending Loading of MPC Wood Truss Splice Joints

As noted by Wolfe et al. (1991), the first step in developing an acceptable design methodology for combined loading is to adopt a standard test procedure. The ANSI/TPI 1-1995 "Standard Method of Test for Strength Properties of Metal Connector Plates Under Pure Tension Forces" describes procedures for determining the steel net-section capacity of splice joints subjected to tension only. This tension-only test standard could be easily modified to create a standard method for testing splice joints in combined tension and bending. Based on the experience gained from the research conducted for this thesis, some recommendations for creating such a standard are given here.

First, the length of the test specimens should be 44 in. This length was used for the specimens of this study, and is recommended for several reasons. This length allows two specimens to be fabricated from an 8-ft. length of lumber, with sufficient allowances for saw kerf as well as for a one-in. block to be cut from the middle of each specimen. This block can later be used to determine the moisture content and specific gravity of the lumber used. The 44-in. specimen length minimizes the transverse deflection of the specimen caused by the induced bending moment. Lateral deflection at the joint reduces the load eccentricity and thus the moment at the joint, and is more pronounced for longer members. Also, most universal testing machines should easily accommodate the 44-in. specimen length. Finally, this length makes it relatively easy for one technician to handle the test specimen.

The truss plates used should be of sufficient length to cause failures in the steel net-section. If necessary, the ends of the plates could be clamped as outlined in the ANSI/TPI tension-only test method.

Five specimens should be tested for each joint configuration (i.e., plate type and grade, and lumber size, grade, and species). The ANSI/TPI standard for tension-only tests requires six replicates to be tested; considering the consistent results of the tests in this study even when only three replicates were successfully tested, testing six replicates (and perhaps even five) seems unnecessary. In addition, when testing truss joints to determine the lateral resistance ("tooth-withdrawal") strength according to the applicable ANSI/TPI standard, only five replicates are necessary. This seems contradictory, considering that more wood-related factors affect tooth-withdrawal strength than affect steel net-section capacity, and that wood has more natural variability than steel.

Extra test specimens should be fabricated in case of any unforeseen events that may cause some of the test data to be suspect, and therefore not reliable for subsequent use. In this study, the problem with the initial design of the grip plates that caused tension perpendicular-to-grain failures in the lumber at the bolts, and the problem with the LVDT setup both resulted in a loss of

data from test replicates. Thus, it is recommended that *twice* the required number of specimens be fabricated when testing truss splice joints in combined loading.

To produce both tension and moment in the splice joint, eccentric axial loading should be applied to both ends of the test specimen. The grip plates designed and used in this study performed adequately; a similar grip plate design is recommended. To protect the test machine from any side loads (perpendicular to the load piston) that may result from the eccentric loading, a universal joint may be located between the grip plates and the load piston.

The levels of initial eccentricity used in this study provided a good range of tension-to-moment ratios. The 1.5-in. initial eccentricity produced ultimate tension loads that were about two-thirds of the ultimate tension-only capacity. The 3.0 and 3.5-in. initial eccentricities produced ultimate tension loads that were about one-third of the ultimate tension-only capacity. The 4.5-in. initial eccentricity for the 2x4 joints produced ultimate tension loads that were about one-fourth of the ultimate tension-only capacity. Thus, for a recommended specimen length of 44 in., initial eccentricities should be similar to those used in this study. In addition, a very low initial eccentricity, such as 0.5 or 1.0 in., would provide a large tension with a relatively low moment and is recommended.

The transverse deflection, Δ, of the splice joint caused by the bending moment must be measured so that the actual moment at failure may be calculated. An LVDT or other such device is recommended for measuring the transverse deflection. The actual moment at failure, M, can be calculated using Equation 5.25:

$$M = T(e-\Delta) \qquad (5.25)$$

where T is the measured tension at failure and e is the initial eccentricity.

The joint gap should be measured prior to testing the specimen. The gap on both sides of the joint should be measured, and recorded as the tension-side gap and the compression-side gap. This data may be used to determine if the amount of joint gap has any effect on the ultimate moment, similar to the analysis of the joint gap conducted earlier in Section 4.5 of this thesis.

The selected rate of load application should result in times to failure of 3 to 5 minutes, similar to the requirements of the tension-only test standard.

These recommendations are based on testing the joints used in this study as well as the review of test reports by Wolfe (1990) and Gupta (1994). In addition to the above recommendations, any applicable portions of the tension-only standard should be incorporated into the standard test method. It is suggested that these recommendations and the existing tension-only test standard be used to develop a standard method of test for splice joints subjected to combined tension and bending loading.

6. Summary and Conclusions

6.1 Summary

Typical 2x4 and 2x6 bottom chord splice joints of MPC wood trusses were tested in combined tension and bending loading by applying eccentric axial loads to the splice joints. The lumber used for the test joints was No. 2 KD19 Southern Pine. The truss plates used for the 2x4 joints were 3.28 in. wide and 8.75 in. long, and were fabricated from 20-gauge ASTM A653 HSLA Grade 60 steel. Two types of truss plates were used for the 2x6 joints; 5.25- by 10.5-in. plates of 20-gauge ASTM A653 HSLA Grade 60 steel, and 5- by 10.5-in. plates of 16-gauge ASTM A653 SQ Grade 37 steel.

The data generated from these tests were used to evaluate three structural models for predicting the ultimate tensile strength of the steel net-section of the joints tested. In addition to the data from the tests of this study, test data from a previous study of combined loading in splice joints, and test data from a study of bending-only in splice joints were used to evaluate the models. Of the three models evaluated, Model 2 was validated based on the performance of the model in predicting the ultimate moment capacities.

A design procedure based on Model 2 was developed for determining the allowable design strength of the steel net-section of splice joints subjected to combined tension and bending loading. The new design procedure was compared with two alternative design methods. One design method shown in the ANSI/TPI 1-1995 Commentary compared well with the new proposed method.

6.1.1 Summary of the Proposed Design Procedure

To determine the allowable design capacity of the steel net-section of a bottom chord splice joint subjected to combined tension and bending loading, a pair of truss plates for the splice joint are selected. Next, the median value of the ultimate compressive strength of the wood for loading parallel-to-grain, $\tilde{C}$, is estimated using Equation 6.1:

$$\tilde{C} = 1.36(1.9 C_F F_c) \tag{6.1}$$

where F_c, the nominal design value for compression parallel-to-grain, and C_F, the size factor for compression parallel-to-grain, are the appropriate values for the species and grade of lumber used. F_c and C_F for grades and species are tabulated in the NDS Supplement (AFPA, 1991).

Next, Equations 6.2 and 6.3 are solved simultaneously using the plate properties and the applied moment, M (determined from the engineering analysis of the truss), to determine y, the location of the neutral axis, and T_{ult}, the ultimate tension load that will cause steel net-section failure of the joint when applied in conjunction with the applied moment, M.

$$y = \frac{\frac{1}{4} bd\tilde{C} + T_{ult} - twe_t F_u}{2te_t F_u + \frac{1}{2} b\tilde{C}} \tag{6.2}$$

$$M + T_{ult} y = te_t F_u (\tfrac{1}{2} w + y)^2 + \tfrac{1}{3} b\tilde{C}(\tfrac{1}{2} d - y)^2 \tag{6.3}$$

The location of the neutral axis, y, must lie within the truss plate. Equation 6.4 is used for this check:

$$|y| \le \tfrac{1}{2} w \tag{6.4}$$

Using Equation 6.5, the allowable tension load, $T_{all,M}$, that may be safely applied when the applied moment, M, is present is calculated as:

$$T_{all,M} = 0.5\, T_{ult} \tag{6.5}$$

The allowable tension-only capacity of the steel net-section of the truss plates, $T_{all,T}$, is calculated using Equation 6.6:

$$T_{all,T} = 2tw(0.6F_y)e_t \tag{6.6}$$

The allowable tension load, T_{all}, is then equal to the minimum of $T_{all,M}$ and $T_{all,T}$, as shown by Equation 6.7:

$$T_{all} = \min\begin{cases} T_{all,M} \\ T_{all,T} \end{cases} \tag{6.7}$$

The applied tension load, T, determined from the engineering analysis of the truss, must not exceed T_{all}:

$$T \le T_{all}$$

Next, M_{ult}, the ultimate moment-only capacity of the steel net-section of the truss plates, can be determined by solving Equations 6.8 and 6.9:

$$y^* = \frac{¼\,bd\tilde{C} - twe_t F_u}{2te_t F_u + ½\,b\tilde{C}} \tag{6.8}$$

$$M_{ult} = te_t F_u (½\,w + y^*)^2 + ⅓\,b\tilde{C}(½\,d - y^*)^2 \tag{6.9}$$

The location of the neutral axis, y^*, must lie within the truss plate. Equation 6.10 is used to check this:

$$|y^*| \le ½\,w \tag{6.10}$$

The allowable moment, M_{all}, is determined using Equation 6.11:

$$M_{all} = 0.5\,M_{ult} \tag{6.11}$$

Finally, the applied moment, M, must not exceed the allowable moment, M_{all}:

$$M \le M_{all}$$

If either the applied tension or the applied moment is greater than their respective allowable values, then the steel net-section of the selected truss plates is inadequate.

In addition to the design checks for the steel net-section capacity of a splice joint summarized by Equations 6.1 through 6.11, the design check for the tooth withdrawal capacity is always required.

6.2 Conclusions

The conclusions from this study were:

1. Applying an eccentric axial load to a splice joint test specimen is a simple, effective, and consistent method of producing combined tension and bending stresses at the splice joint.

2. Model 2, defined by Equations 5.4 and 5.5, is an accurate model for predicting the ultimate moment capacity of the steel net-section of splice joints subjected to combined tension and bending.

3. The proposed design procedure, given by Equations 6.1-6.11, is recommended for determining the allowable design strength of the steel net-section of splice joints subjected to combined tension and bending loading.

4. The design method given in the Commentary to ANSI/TPI 1-1995 (as modified in this thesis) is a good approximate method for determining the allowable design strength of the steel net-section of splice joints subjected to combined tension and bending loading. This simple method can be used to quickly calculate an estimate of the allowable design strength of a bottom chord splice joint using a hand-held calculator.

6.3 Model Limitations and Recommendations for Future Research

Future research studies of combined tension and bending loading in bottom chord splice joints of MPC wood trusses should use test methods similar to those used and recommended in this study; these methods proved to be simple and effective. In future studies, splice joints of 2x8 and larger lumber sizes should be investigated to validate the accuracy of the proposed model for these lumber sizes. The data from Soltis's (1985) study of splice joints did include 2x8 and 2x10 lumber; however, these joints were tested in bending-only, not combined tension and bending. Nonetheless, the selected structural model, Model 2, was derived using generalized truss plate and lumber dimensions, and thus the proposed design procedure based on this model should be applicable for any lumber size. Tests of 2x10 or 2x12 joints would validate Model 2 for the wide widths of lumber.

None of the truss plates used in this study, or the two previous studies from which data were taken, had "aligned" tooth patterns. However, it is assumed that Model 2 and the proposed design method apply to truss joints with aligned tooth patterns because the tension efficiency ratio includes the effect of tooth pattern on the steel net-section strength of the truss plate. Model 2 could be validated for truss plates with a typical aligned tooth pattern by testing a sample of 2x4 joints and the widest plate/lumber configuration common in the industry.

The model and design procedure were developed with the assumption that the neutral axis lies within the truss plate. If the calculated location of the neutral axis is not within the truss plate the model and design equations are invalid for that particular splice joint. For most typical splice joints with typical loads, the neutral axis will lie within the truss plate. The model and design equation could be modified to use the assumption that the neutral axis lies outside the truss plate. Users of the proposed design procedure should check the position of the neutral axis, an if it does not lie within the truss plate, the 3M/2w procedure can be used to check the steel net-section.

References

American Forest & Paper Association (AF&PA). 1991. National design specification for wood construction supplement: Design values for wood construction. American Forest & Paper Association, Washington, D.C.

American Society of Civil Engineers (ASCE). 1986. Structural wood research needs. *Journal of Structural Engineering* 112(ST9):2155-2165.

American Society of Testing and Materials (ASTM). 1996a. *Test method for tension testing of metallic materials - ASTM E 8-96*. ASTM, Philadelphia, Pa.

ASTM. 1996b. *Standard specification for steel sheet, zinc-coated (galvanized) or zinc-iron alloy-coated (galvannealed) by the hot-dip process - ASTM A 653-96*. ASTM, Philadelphia, Pa.

ASTM. 1996c. *Test method for direct moisture content measurement of wood and wood-based materials - ASTM D 4442-96*. ASTM, Philadelphia, Pa.

ASTM. 1996d. *Test method for specific gravity of wood and wood-based materials - ASTM D 2395-96*. ASTM, Philadelphia, Pa.

ASTM. 1996e. *Establishing allowable properties for visually-graded dimension lumber from in-grade tests of full-size specimens - ASTM D 1990-96a*. ASTM, Philadelphia, Pa.

ASTM. 1994. *Standard specification for steel sheet, zinc-coated (galvanized) by the hot-dip process, structural (physical) quality - ASTM A 446-94*. ASTM, Philadelphia, Pa.

Dudley, H.T. 1966. Determination of net-section properties of metal truss plates. *Forest Products Journal* 16(5):48-49.

Edlund, G. 1971. Butt splicing of timber members with nail plates. Swedish Institute for Wood Technology Research, Report R40, Stockholm, Sweden.

Green, D.W., and J.W. Evans. 1987. Mechanical properties of visually graded lumber: Volume 1, A Summary. USDA Forest service, Forest Products Laboratory, Madison, Wis.

Gupta, R. 1994. Metal-plate connected tension joints under different loading combinations. *Wood and Fiber Science* 26(2):212-222.

Gupta, R., M. Vatovec, and T.H. Miller. 1996. Metal-plate-connected wood joints: a literature review. Forest Research Laboratory, Oregon State University, Corvallis, Oregon. Research Contribution 13.

ICBO Evaluation Service, Inc. 1992a. Evaluation Report No. 3777.

ICBO Evaluation Service, Inc. 1992b. Evaluation Report No. 1591.

Kennedy, D.J.L., and M.M.A. Gad Aly. 1980. Limit states design of steel structures performance factors. *Canadian Journal of Structural Engineering* 7:45-77.

Kevarinmäki, A. 1996. Moment capacity and stiffness of punched metal plate fastener joints. In *Proceedings of the International Wood Engineering Conference* 1:385-392.

Minitab, Inc. 1995. Minitab Release 10.5 Xtra for Windows. Minitab, Inc., State College, Pa.

Noguchi, M. 1980. Ultimate resisting moment of butt joints with plate connectors stressed in bending. *Wood Science* 12(3):168-175.

SBCCI Public Safety Testing and Evaluation Services, Inc. (SBCCI PST & ESI). 1995. Evaluation Report #94168. SBCCI PST & ESI, Birmingham, Alabama.

Segui, W.T. 1994. LRFD steel design. PWS Publishing Company, Boston, Mass.

Skaggs, T. D., F. E. Woeste, and S. L. Lewis. 1995. Steel properties used to manufacture wood truss metal connector plates. Transactions of the ASAE 38(1):187-195.

Soltis, L. A. 1985. Partially continuous floor joists. Research Paper FPL-461. USDA Forest Products Laboratory, Madison, Wi.

Truss Plate Institute (TPI). 1995a. National design standard for metal plate connected wood truss construction. ANSI/TPI 1-1995. Truss Plate Institute, Madison, Wi.

TPI. 1995b. Commentary and appendices to ANSI/TPI 1-1995 National design standard for metal plate connected wood truss construction. Truss Plate Institute, Madison, Wi.

Whale, L.R.J. 1993. Truss plate design: a European overview. In *Proceedings, International Workshop on Wood Connections*. Forest Products Society, Madison Wi.

Wolfe, R. W. 1990. Metal-plate connections loaded in combined bending and tension. *Forest Products Journal* 40(9):17-23.

Wolfe, R. W., M. Hall, and D. Lyles. 1991. Test apparatus for simulating interactive loads on metal plate wood connections. *Journal of Testing and Evaluation*, 19(6):421-428.

Appendix A

Derivation of the Design Method for Splice Joints in the ANSI/TPI 1-1995 Commentary

In this appendix, the derivation of the design method (Equation 2.1) for the steel net-section of tension splice joints given in the ANSI/TPI 1-1995 Commentary is presented. The basic idea of this design method is to convert an applied moment, M, into an equivalent tension force, T^*. This tension force, T^*, can then be added to the applied tension force, T, and the resulting total force is used to design the steel net-section of the joint. The first step in deriving this design method is to consider the stress distribution shown in Figure A.1. A bending moment is applied to a member with a rectangular cross-section. Assuming that the member behaves elastically, the applied moment M will produce a linear stress distribution. Equation A.1 gives the stress at the extreme edges of the member:

$$\sigma_M = \frac{M}{S} = \frac{M}{\frac{bd^2}{6}} = \frac{6M}{bd^2} \qquad \text{(A.1)}$$

where S is the section modulus of a rectangular cross-section, and b and d are the thickness and depth of the member, respectively.

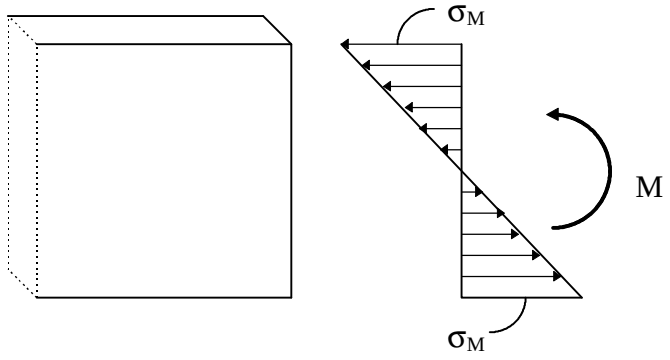

Figure A.1 Stress distribution for a member subjected to moment, M.

The moment can be transformed into an equivalent force couple, as shown in Figure A.2, where d is the depth of the member, and σ_M is the maximum stress in the member caused by the moment:

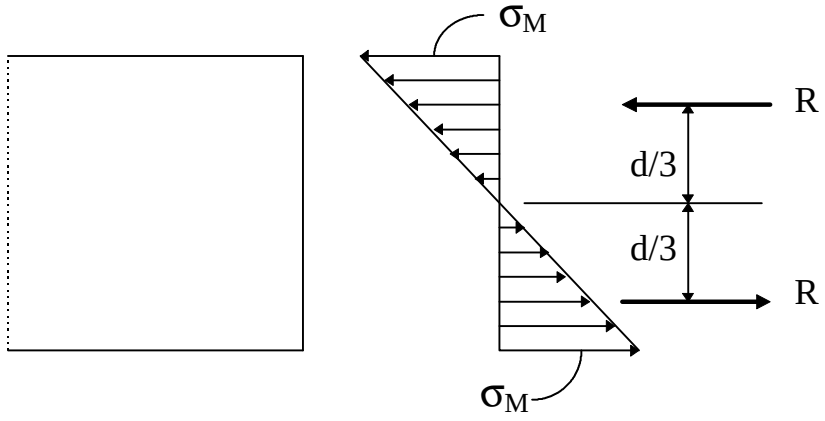

Figure A.2 Force couple equivalent to moment M.

The two forces, each acting at a distance of one-third of the member depth from the centerline of the member, will produce the same stress distribution as the applied moment M. Equation A.2 gives the relationship between R and M:

$$R = \frac{3M}{2d} \qquad (A.2)$$

This equation can be easily found by summing moments about the centerline of the member, setting them equal to M, and then solving for R.

The next step in the derivation of this design method is to use the force, R, as the equivalent tension force, T^*. This force is then applied across the entire cross-section of the member, in the same manner a tension force would be applied. However, applying this force as an equivalent tension force does not produce the same maximum stress that the applied moment M produces. This outcome can be demonstrated by considering Figure A.3, where the "equivalent" tension force T^* is assumed equal to R, and is applied to the same member.

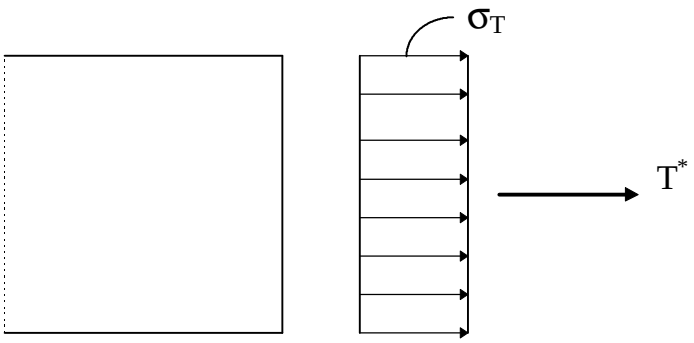

Figure A.3 Stress distribution for equivalent tension force, T^*.

The stress produced, σ_T, is given by Equation A.3:

$$\sigma_T = \frac{T^*}{A} \tag{A.3}$$

where A is the cross-sectional area of the member. Since T^* is equal to R, Equation A.2 can be substituted for T^* in Equation A.3, and then Equation A.4 results:

$$\sigma_T = \frac{T^*}{A} = \frac{\frac{3M}{2d}}{A} = \frac{\frac{3M}{2d}}{bd} = \frac{3M}{2bd^2} = \frac{1.5M}{bd^2} \tag{A.4}$$

If the goal were to find a tension force, T^*, that would produce a maximum stress equivalent to the maximum stress caused by the applied moment M, then the stresses given in Equations A.1 and A.4 should be equivalent. However, it is obvious that they are not equal; in fact, the stress produced by the "equivalent" tension force is only one-forth of the stress produced by the applied moment. The discrepancy results from using R as the equivalent force T^*.

When R acts as a force couple, as shown in Figure A.2, it does produces the same stress distribution as the applied moment M. But when R is applied as an axial force, it does not give the same maximum stress as M. In addition to the use of a simple rule (which is not based on statics and linear stress theory) of using R as the equivalent tension force and applying it over the entire cross-section, the assumption is made that the member has a solid rectangular cross-section,

which must be accounted for by the steel efficiency ratio, e_t. Using R as the equivalent force applied across the entire cross-section may balance out the differences in net-section moment capacity due to non-linear material behavior versus the idealized linear stress distribution model of Equation A.1. This may also explain why this design method yields similar designs as the method developed in this thesis.

Appendix B

Tables of Ratios of the Median to the Fifth Percentile of the Compression Parallel-To-Grain Strength for Five Species Groups of Dimension Lumber, Adapted from Green and Evans (1987)

Table B.1 Summary of compression property estimates for Douglas Fir-Larch lumber, adapted from Green and Evans (1987).

Moisture Content (%)	Lumber Size	Grade	Sample Size	Compressive Strength (psi) Median	Fifth Percentile	Ratio of Median to Fifth Percentile
12	2x4	Select Str.	390	6,166	4,628	1.33
12	2x4	No. 1 & Btr	389	5,615	3,996	1.41
12	2x4	No. 2	385	4,861	3,383	1.44
12	2x8	Select Str.	358	5,585	3,940	1.42
12	2x8	No. 1 & Btr	362	5,135	3,492	1.47
12	2x8	No. 2	353	4,215	2,766	1.52
12	2x10	Select Str.	359	5,302	3,806	1.39
12	2x10	No. 1 & Btr	354	4,957	3,525	1.41
12	2x10	No. 2	350	4,409	2,817	1.57
15	2x4	Select Str.	390	5,313	4,096	1.30
15	2x4	No. 1 & Btr	389	4,872	3,603	1.35
15	2x4	No. 2	385	4,278	3,123	1.37
15	2x8	Select Str.	358	4,848	3,560	1.36
15	2x8	No. 1 & Btr	362	4,494	3,209	1.40
15	2x8	No. 2	353	3,774	2,643	1.43
15	2x10	Select Str.	359	4,624	3,455	1.34
15	2x10	No. 1 & Btr	354	4,354	3,234	1.35
15	2x10	No. 2	350	3,925	2,675	1.47
					Average	**1.41**

Table B.2 Summary of compression property estimates for Douglas Fir (South) lumber, adapted from Green and Evans (1987).

Moisture Content (%)	Lumber Size	Grade	Sample Size	Compressive Strength (psi) Median	Fifth Percentile	Ratio of Median to Fifth Percentile
12	2x4	Select Str.	84	5,801	4,497	1.29
12	2x4	No. 1 & Btr	80	5,403	4,272	1.26
12	2x4	No. 2	86	4,448	3,512	1.27
12	2x8	Select Str.	38	5,566	3,958	1.41
12	2x8	No. 1 & Btr	38	4,987	3,273	1.52
12	2x8	No. 2	43	3,934	2,617	1.50
12	2x10	Select Str.	42	4,592	3,509	1.31
12	2x10	No. 1 & Btr	40	4,450	3,496	1.27
12	2x10	No. 2	42	4,022	2,780	1.45
15	2x4	Select Str.	84	5,000	3,967	1.26
15	2x4	No. 1 & Btr	80	4,680	3,791	1.23
15	2x4	No. 2	86	3,927	3,198	1.23
15	2x8	Select Str.	38	4,811	3,545	1.36
15	2x8	No. 1 & Btr	38	4,350	3,010	1.45
15	2x8	No. 2	43	3,527	2,491	1.42
15	2x10	Select Str.	42	4,039	3,195	1.26
15	2x10	No. 1 & Btr	40	3,929	3,185	1.23
15	2x10	No. 2	42	3,595	2,620	1.37
					Average	**1.34**

Table B.3 Summary of compression property estimates for Hem-Fir lumber, adapted from Green and Evans (1987).

Moisture Content (%)	Lumber Size	Grade	Sample Size	Compressive Strength (psi) Median	Fifth Percentile	Ratio of Median to Fifth Percentile
12	2x4	Select Str.	410	5,280	3,994	1.32
12	2x4	No. 1 & Btr	410	4,765	3,474	1.37
12	2x4	No. 2	402	4,186	3,100	1.35
12	2x8	Select Str.	327	4,715	3,442	1.37
12	2x8	No. 1 & Btr	328	4,374	3,088	1.42
12	2x8	No. 2	326	4,000	2,695	1.48
12	2x10	Select Str.	290	4,629	3,484	1.33
12	2x10	No. 1 & Btr	291	4,395	3,161	1.39
12	2x10	No. 2	302	3,812	2,702	1.41
15	2x4	Select Str.	410	4,555	3,536	1.29
15	2x4	No. 1 & Btr	410	4,142	3,131	1.32
15	2x4	No. 2	402	3,687	2,839	1.30
15	2x8	Select Str.	327	4,102	3,107	1.32
15	2x8	No. 1 & Btr	328	3,835	2,830	1.36
15	2x8	No. 2	326	3,542	2,520	1.41
15	2x10	Select Str.	290	4,035	3,139	1.29
15	2x10	No. 1 & Btr	291	3,851	2,886	1.33
15	2x10	No. 2	302	3,395	2,527	1.34
					Average	**1.36**

Table B.4 Summary of compression property estimates for Mixed Southern Pine lumber, adapted from Green and Evans (1987).

Moisture Content (%)	Lumber Size	Grade	Sample Size	Compressive Strength (psi) Median	Fifth Percentile	Ratio of Median to Fifth Percentile
12	2x4	Select Str.	166	5,627	4,194	1.34
12	2x4	No. 1 & Btr	161	5,366	4,160	1.29
12	2x4	No. 2	156	4,641	3,436	1.35
12	2x6	Select Str.	151	5,134	3,980	1.29
12	2x6	No. 1 & Btr	134	4,955	3,914	1.27
12	2x6	No. 2	142	4,517	3,327	1.36
12	2x8	Select Str.	162	4,812	3,468	1.39
12	2x8	No. 1 & Btr	134	4,769	3,459	1.38
12	2x8	No. 2	166	4,122	2,947	1.40
15	2x4	Select Str.	166	4,851	3,718	1.30
15	2x4	No. 1 & Btr	161	4,641	3,691	1.26
15	2x4	No. 2	156	4,067	3,127	1.30
15	2x6	Select Str.	151	4,456	3,550	1.26
15	2x6	No. 1 & Btr	134	4,314	3,498	1.23
15	2x6	No. 2	142	3,970	3,041	1.31
15	2x8	Select Str.	162	4,201	3,151	1.33
15	2x8	No. 1 & Btr	134	4,168	3,144	1.33
15	2x8	No. 2	166	3,661	2,742	1.34
					Average	**1.32**

Table B.5 Summary of compression property estimates for Southern Pine lumber, adapted from Green and Evans (1987).

Moisture Content (%)	Lumber Size	Grade	Sample Size	Compressive Strength (psi) Median	Fifth Percentile	Ratio of Median to Fifth Percentile
12	2x4	Select Str.	419	6,544	4,792	1.37
12	2x4	No. 1 & Btr	412	6,251	4,350	1.44
12	2x4	No. 2	428	4,653	3,453	1.35
12	2x8	Select Str.	429	6,003	4,189	1.43
12	2x8	No. 1 & Btr	412	5,858	3,943	1.49
12	2x8	No. 2	428	4,397	3,183	1.38
12	2x10	Select Str.	427	5,715	4,303	1.33
12	2x10	No. 1 & Btr	412	5,681	4,209	1.35
12	2x10	No. 2	430	4,584	3,036	1.51
15	2x4	Select Str.	419	5,636	4,248	1.33
15	2x4	No. 1 & Btr	412	5,399	3,903	1.38
15	2x4	No. 2	428	4,139	3,201	1.29
15	2x8	Select Str.	429	5,200	3,777	1.38
15	2x8	No. 1 & Btr	412	5,085	3,585	1.42
15	2x8	No. 2	428	3,940	2,988	1.32
15	2x10	Select Str.	427	4,972	3,866	1.29
15	2x10	No. 1 & Btr	412	4,944	3,793	1.30
15	2x10	No. 2	430	4,085	2,871	1.42
					Average	**1.38**

Vita

On September 16, 1972, the fourth child and only son of Jack and Nevvile O'Regan was born. Philip J. O'Regan developed his technical skills as a young boy by patiently handing tools to his father whose head was buried under the hood of the family car. Soon bored with simply handing tools and looking for dropped parts in the dirt, Phil began asking questions, which his father patiently and thoroughly answered. Thus began the inquisitive thinking that would lead Phil to become a student of engineering.

Phil enrolled in Virginia Tech in the Fall of 1990, and eventually received his Bachelor's degree in Agricultural Engineering in December, 1995. He stayed in Blacksburg and began work on a Master's degree the following semester. Phil was a member of the American Society of Agricultural Engineers, the National Society of Professional Engineers, and the Forest Products Society. As a graduate student, Phil was invited to join the honor societies of Alpha Epsilon and Gamma Sigma Delta.